

Supplementary Information

Dual superlyophobic surfaces with superhydrophobicity and underwater superoleophobicity

Lu Tie,^{a,c} Jing Li,^{a,*} Mingming Liu,^{a,c} Zhiguang Guo,^{a,b,*} Yongmin Liang,^{a,d} and Weimin Liu^{a,*}

^a State Key Laboratory of Solid Lubrication, Lanzhou Institute of Chemical Physics, Chinese Academy of Sciences, Lanzhou 730000, People's Republic of China

^b Ministry of Education Key Laboratory for the Green Preparation and Application of Functional Materials, Hubei University, Wuhan 430062, People's Republic of China

^c University of Chinese Academy of Sciences, Beijing 100049, People's Republic of China

^d State Key Laboratory of Applied Organic Chemistry, Lanzhou University, Lanzhou 730000, People's Republic of China

*E-mail: jli@licp.cas.cn (J. Li); zguo@licp.cas.cn (Z. Guo); wmliu@licp.cas.cn (W. Liu).

Table of Contents

Supplementary Section 1: Methods	4
Materials	4
Preparation of dual superlyophobic fabric and sponge.....	4
Preparation of dual superlyophobic nickel foam and zinc sheet	4
Preparation of dual superlyophobic copper sheet.....	4
Preparation of dual superlyophobic SSM.....	5
Oil-water separation.....	5
Characterization.....	6
Supplementary Section 2: Beetle's back	7
Figure S1. Surface structures of the beetle's back.....	7
Supplementary Section 3: Dual superlyophobic fabric	7
Figure S2. Photographs of the fabric samples.	7
Figure S3. SEM images of original fabric	7
Figure S4-S9. Wetting properties of the fabric samples	8-10
Figure S10,S11. EDS analysis of the fabric samples.....	10,11
Figure S12,S13. XPS spectra of the fabric samples	12,13
Supplementary Section 4: Dual superlyophobic sponge	13
Figure S14. Photographs of the sponge samples	13
Figure S15. SEM images of the sponge samples.....	14
Figure S16. Wetting properties of the sponge samples.....	14
Figure S17,S18. EDS analysis of dual superlyophobic sponge.....	15
Figure S19. XPS spectra of the fabric samples.....	16
Supplementary Section 5: Dual superlyophobic nickel foam	16
Figure S20. Photographs of the nickel foam samples.....	16
Figure S21. SEM images of the nickel foam samples	17
Figure S22. Wetting properties of the nickel foam samples	17
Figure S23,S24. EDS analysis of dual superlyophobic nickel foam	18
Figure S25. XPS spectra of the nickel foam samples.....	19
Supplementary Section 6: Dual superlyophobic zinc sheet	19
Figure S26. Photographs of the zinc sheet samples.....	20

Figure S27. SEM images of the zinc sheet samples	20
Figure S28. Wetting properties of the zinc sheet samples	20
Figure S29,S30. EDS analysis of dual superlyophobic zinc sheet	21
Figure S31. XPS spectra of the zinc sheet samples	22
Figure S32. XRD patterns of the zinc sheet samples.....	22
Supplementary Section 7: Dual superlyophobic copper sheet.....	23
Figure S33. Photographs of the copper sheet samples	23
Figure S34. SEM images of the copper sheet samples	23
Figure S35. Wetting properties of the copper sheet samples	24
Figure S36,S37. EDS analysis of dual superlyophobic copper sheet.....	24,25
Figure S38. XPS spectra of the copper sheet samples.....	26
Figure S39. XRD patterns of the copper sheet samples	26
Supplementary Section 8: Dual superlyophobic SSM.....	27
Figure S40. Photographs of the SSM samples.....	27
Figure S41. SEM images of the SSM samples	28
Figure S42. Wetting properties of the SSM samples	29
Figure S43-S48. EDS analysis of the SSM samples.....	30-34
Figure S49. XPS spectra of the SSM samples	35
Figure S50. XRD patterns of the SSM samples	36
Supplementary Section 9: Oil-water separation	36
Figure S51. Separation of immiscible oil-water mixtures	36
Figure S52-S55. Emulsion separation	37-39
Figure S56,S57. Stability of dual superlyophobic surfaces.....	40
Supplementary Section 10: Thermodynamic analysis.....	41
Figure S58. Theoretical study on flat surfaces	41
Figure S59. Wetting property of the flat modified copper sheet	41
Supplementary Section 11: Movies	42
Movie S1. θ^*_w of CuO-coated fabric.	42
Movie S2. θ^*_w of CuO-coated fabric modified with 0.1 mM n-octadecylthiol.	42
Movie S3. Sliding angles of the dual superlyophobic fabric.....	42
Movie S4,S5. Separation of immiscible oil-water mixtures.....	42

Methods

Materials. Fabric, sponge, nickel foam, zinc sheet, copper sheet, and SSM (2300 mesh size) were commercially available. Diesel was purchased from an adjacent gas station. 1H,1H,2H,2H-Perfluorodecanethiol (97%) and n-octadecylthiol (96%) were obtained from Sigma-Aldrich and Acros Organics, respectively. The beetle was obtained from the Tengger Desert. Its back was observed on a field emission scanning electron microscope.

Preparation of dual superlyophobic fabric and sponge. CuO nanoparticles were first fabricated. Typically, $\text{Cu}(\text{CH}_3\text{CO}_2)_2$ (0.025 mol) and CH_3COOH (0.05 mol) were dissolved in 500 mL anhydrous ethanol. NaOH (0.1 mol) was added to the ethanol solution at 78 °C under stirring. The reaction was conducted for 1 h, getting CuO nanoparticle suspensions. Next, commercial fabric and sponge were washed with ethanol and water. The cleaned fabric and sponge were immersed into the CuO nanoparticle suspensions for 5 min at room temperature followed by drying at 60 °C and washing with water. The dip-coating procedure was repeated for three times. Afterward, the CuO-coated fabric and sponge were immersed into anhydrous ethanol containing 1H,1H,2H,2H-perfluorodecanethiol and n-octadecylthiol at different concentrations for 1 h at room temperature. The modified fabric and sponge were thoroughly washed with anhydrous ethanol to get rid of any residual thiol followed by drying at 60 °C.

Preparation of dual superlyophobic nickel foam and zinc sheet. Nickel foam and zinc sheet were immersed into 100 ml aqueous solution of 0.1 M CuCl_2 and 1 M HCl for 5 s at room temperature. After washing with deionized water and drying at 60 °C, the treated nickel foam and zinc sheet were immersed in 0.2 mM 1H,1H,2H,2H-perfluorodecanethiol anhydrous ethanol solution for 1 h at room temperature. The prepared dual superlyophobic nickel foam and zinc sheet were washed with anhydrous ethanol followed by drying at 60 °C.

Preparation of dual superlyophobic copper sheet. Copper sheet was treated in 20 mL aqueous solution of 1 M CuCl_2 and 1 M HCl for 1 h at 100 °C. After washing with deionized water and drying at 60 °C, the treated copper sheet was immersed in 0.2 mM

1H,1H,2H,2H-perfluorodecanethiol anhydrous ethanol solution for 1 h at room temperature. The prepared dual superlyophobic copper sheet was washed with anhydrous ethanol followed by drying at 60 °C.

Preparation of dual superlyophobic SSM. SSM was immersed in 2 M HCl aqueous solution to remove any surface oxide layer and then cleaned with deionize water. First, an electrochemical deposition method was adopted to coat metallic copper on the SSM surface. SSM, platinum sheet, and saturated calomel electrode were used as the working, counter, and reference electrodes, respectively. Metallic copper was grown under a constant current density of 0.1 mA cm⁻² in 1 M CuSO₄ and 0.1 M H₂SO₄ aqueous solution for 5400 s at room temperature. Next, the Cu-coated SSM was immersed in aqueous solution of 1 M NaOH and 0.05 M K₂S₂O₈ for 1 h at room temperature followed by calcination at 150 °C for 30 min. Finally, the treated SSM was immersed in 0.2 mM 1H,1H,2H,2H-perfluorodecanethiol anhydrous ethanol solution for 1 h at room temperature. The prepared dual superlyophobic SSM was washed with anhydrous ethanol followed by drying at 60 °C.

Oil-water separation. The dual superlyophobic fabric with large pore size was used to separate immiscible oil-water mixtures. The prepared fabric was fixed between two glass tubes that were placed vertically. The immiscible oil-water mixtures (50%, v/v) were poured onto the fabric surface that was only prewetted by water. Oil-in-water emulsions were prepared by mixing water and oil (hexane and toluene) at a volume ratio of 100:1 with addition of 0.1 g/L Tween 80 under sharp stirring. Water-in-oil emulsions were prepared by mixing water and oil (1,2-dichloroethane and chloroform) at a volume ratio of 1:100 with addition of 1 g/L Span 80 under sharp stirring. In addition, diesel-in-water and water-in-diesel emulsions were prepared by mixing water and diesel at a volume ratio of 100:1 and 1:100, respectively. All turbid emulsions were highly stable for 24 h. The dual superlyophobic SSM with small pore size was used to separate the prepared oil-in-water and water-in-oil emulsions under gravity.

Characterization. A digital camera (Sony, DSC-HX200) was used to take all optical photographs. The surface structures were observed on a field emission scanning electron microscope (JEOL, JSM-6701F). The samples were pre-treated by Au-sputtered specimens to increase surface conductivity. The measured accelerating voltage and current were 5 kV and 10 μ A, respectively. The element mapping images were got on a scanning electron microscope (JEOL, JSM-5600LV) by EDS analysis. The chemical compositions were further characterized by XPS (Thermo Scientific ESCALAB 250Xi), in which the binding energy of C 1s (284.8 eV) acted as the reference. XRD was performed on an Analytical X'Pert PRO diffract meter to investigate the crystal structures of samples. CAs were obtained on a JC20001 CA system (Zhongchen digital equipment Co., Ltd. Shanghai, China). Before measuring underwater oil CAs, the samples were prewetted by ethanol and then water. The average CA values were calculated by measuring the sample at five different positions. The volume of liquid droplets was about 5 μ L. An OLYMPUS BX51 microscope was employed to record optical microscope images of emulsions. The organic contents in the collected water were analyzed by measuring COD according to U.S. Environmental Protection Agency method 8000 (HACH, DRB 200). A Karl Fischer titrator (Metrohm 831 KF, Switzerland) was used to detect the purities of the collected oils. The sizes of the feed emulsions were calculated by DLS analysis with a Zetasizer Nano ZS (Malvern 3600, U.K.). All measurements were repeated for 3–5 times and the results were reproducible with relative errors less than $\pm 5\%$.

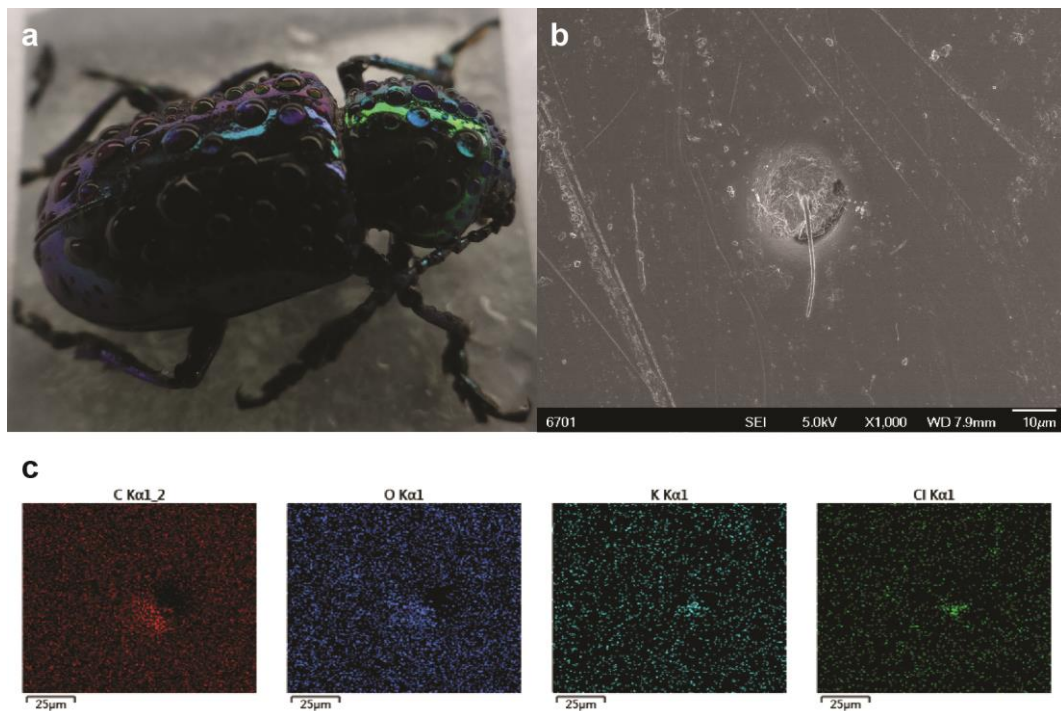


Figure S1. (a) Photograph of the beetle. (b) SEM and (c) the corresponding element mapping images of the beetle's back.

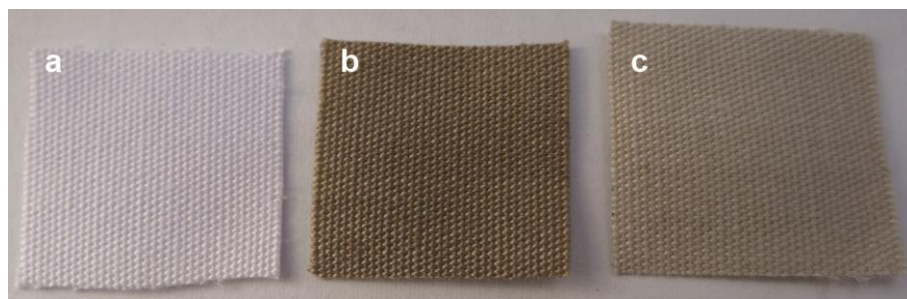


Figure S2. Photographs of original (a) and CuO-coated fabrics modified with 0.2 mM (b) and 15 mM (c) 1H,1H,2H,2H-perfluorodecanethiol.

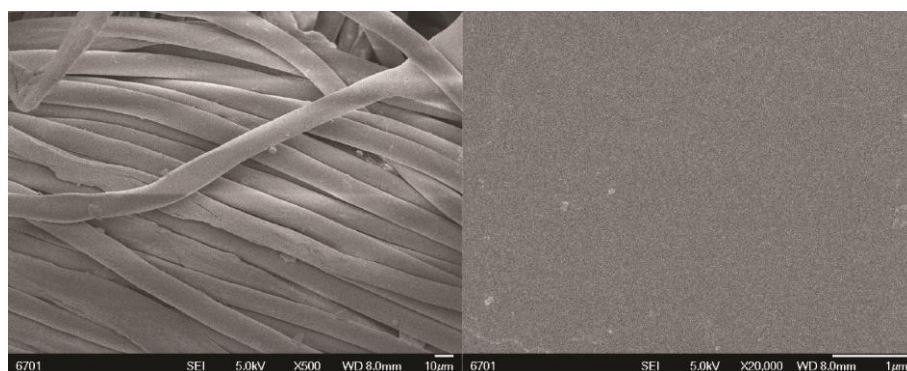


Figure S3. SEM images of original fabric.

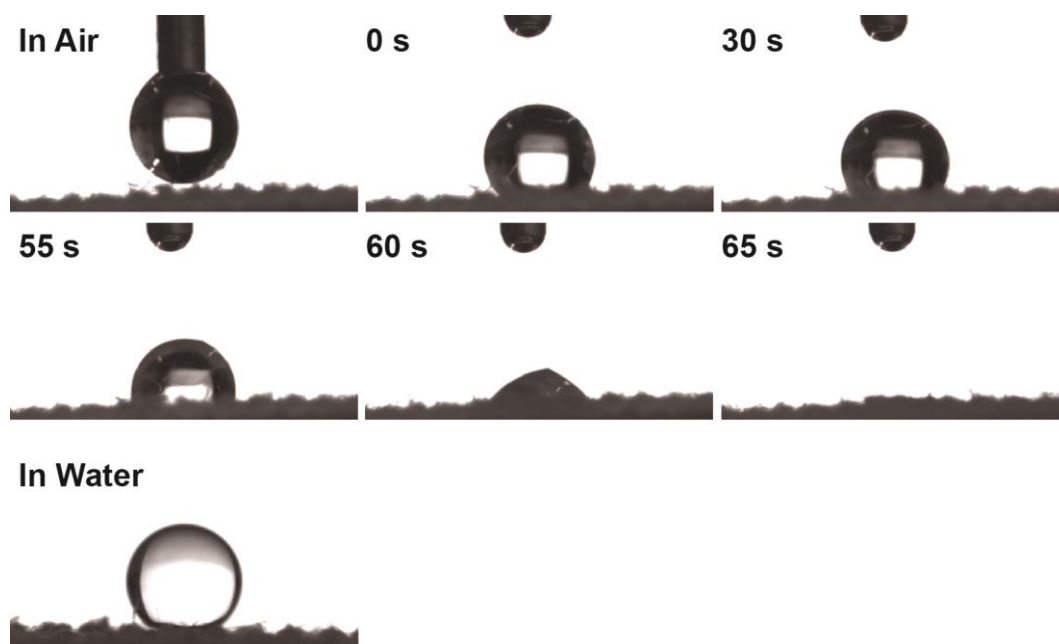


Figure S4. θ^*_w and θ^*_{ow} of original fabric.

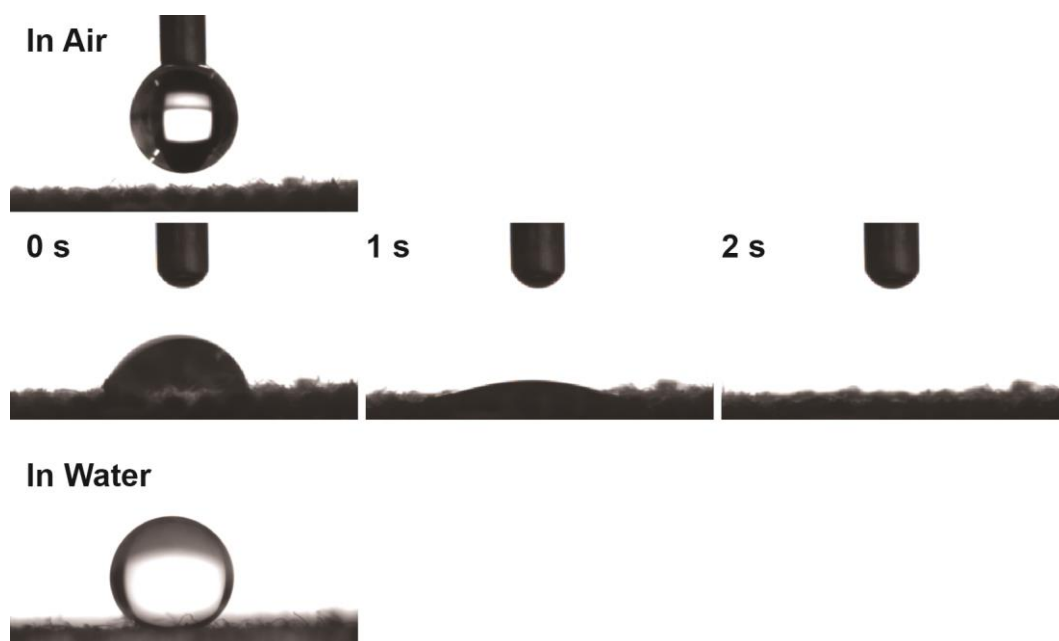


Figure S5. θ^*_w and θ^*_{ow} of CuO-coated fabric.

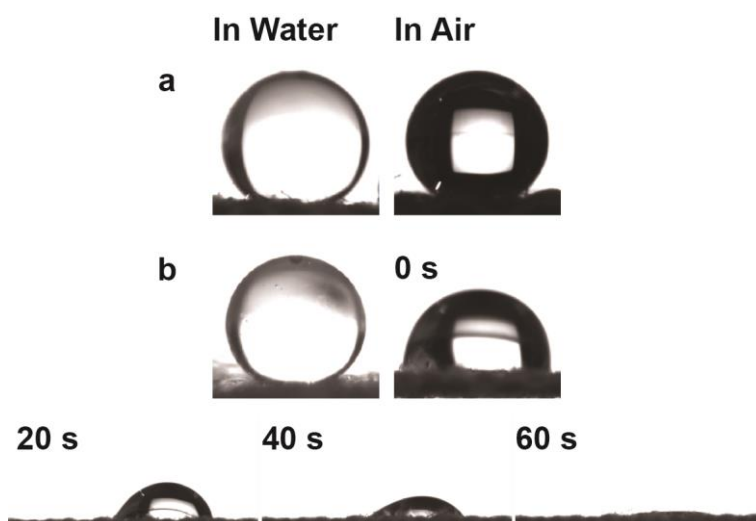


Figure S6. θ^*_w and θ^*_{ow} of CuO-coated fabrics modified with 0.1 mM 1H,1H,2H,2H-perfluorodecanethiol (a) and n-octadecylthiol (b).



Figure S7. θ^*_w and θ^*_{ow} of CuO-coated fabric modified with 0.2 mM n-octadecylthiol.

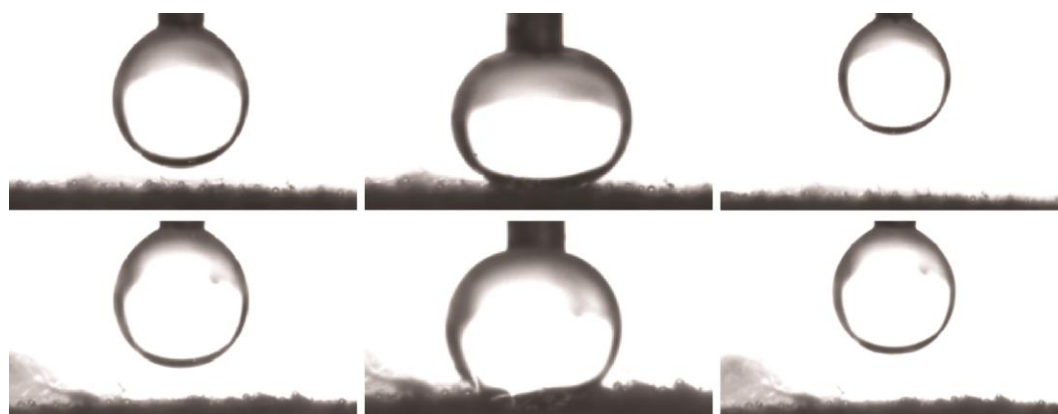


Figure S8. Dynamic adhesion measurements of an oil droplet (1,2-dichloroethane) in water on the surfaces of the prepared fabrics modified with 0.1 mM (upper) and 0.2 mM (below) 1H,1H,2H,2H-perfluorodecanethiol.



Figure S9. A hexane droplet in water on the surface of the prepared fabric modified with 0.2 mM 1H,1H,2H,2H-perfluorodecanethiol. The hexane droplet easily rolls along the inclined surface of the modified fabric.

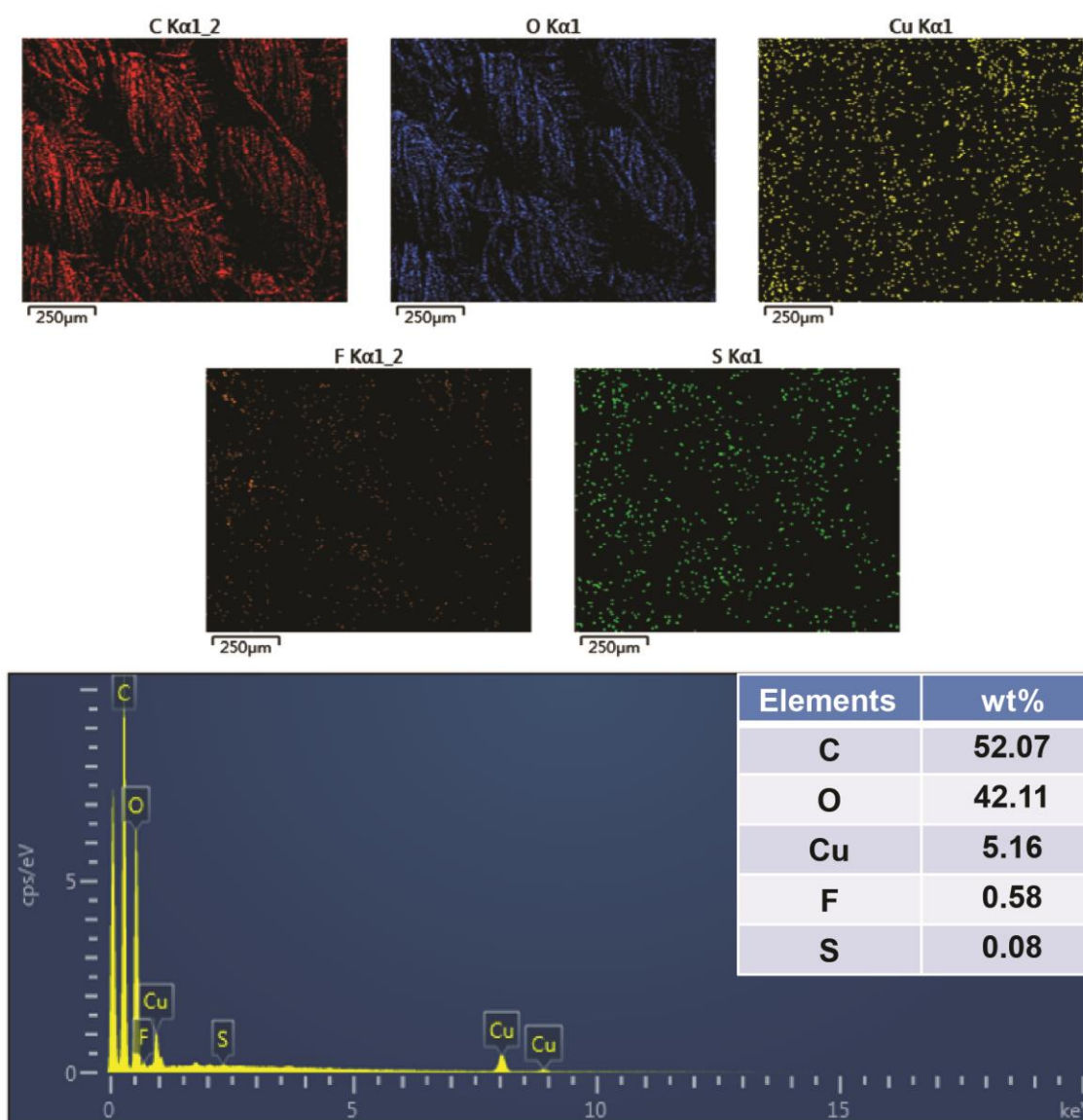


Figure S10. Element mapping images and element percent of the prepared fabric modified with 0.2 mM 1H,1H,2H,2H-perfluorodecanethiol.

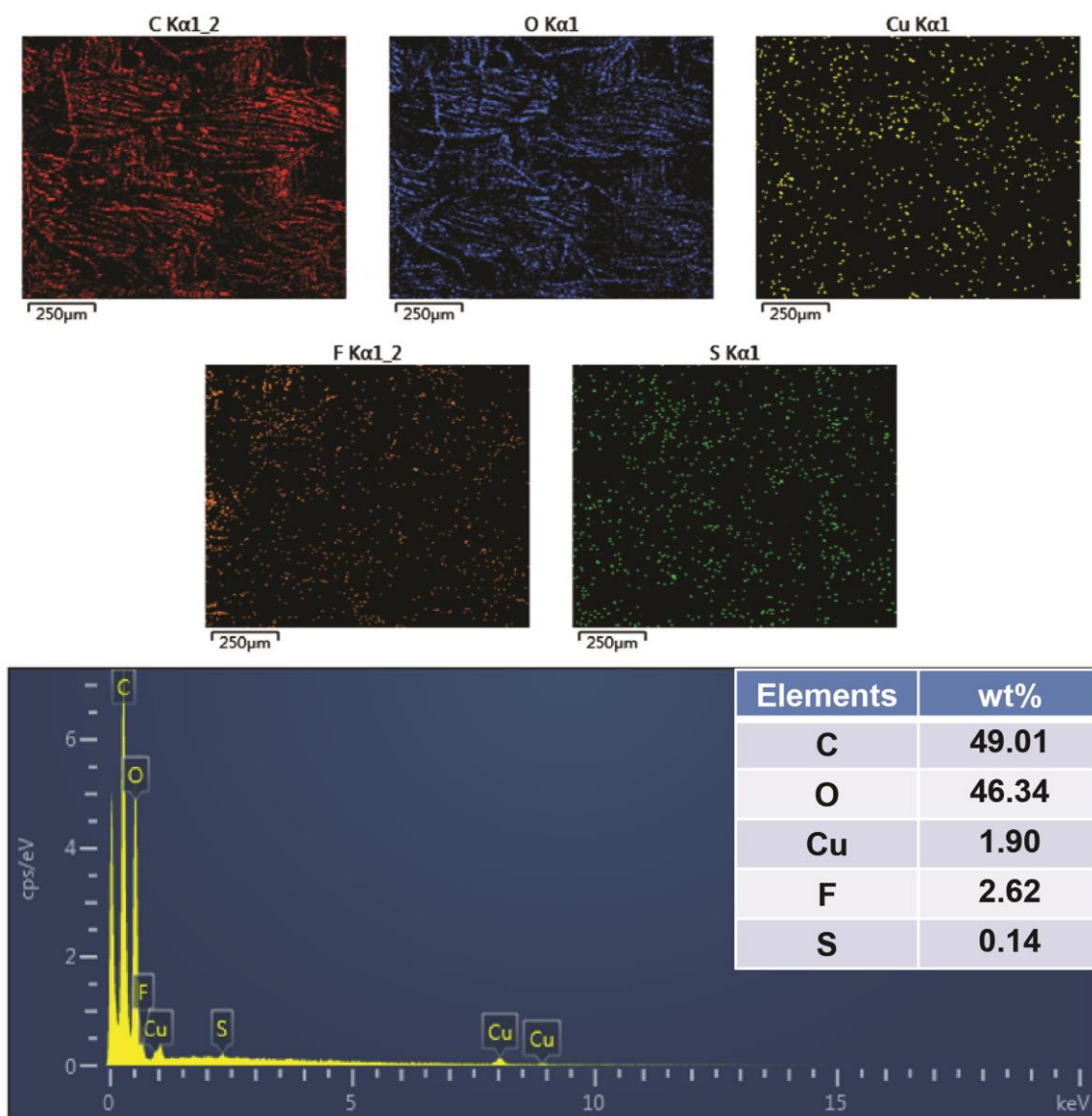


Figure S11. Element mapping images and element percent of the prepared fabric modified with 15 mM 1H,1H,2H,2H-perfluorodecanethiol.

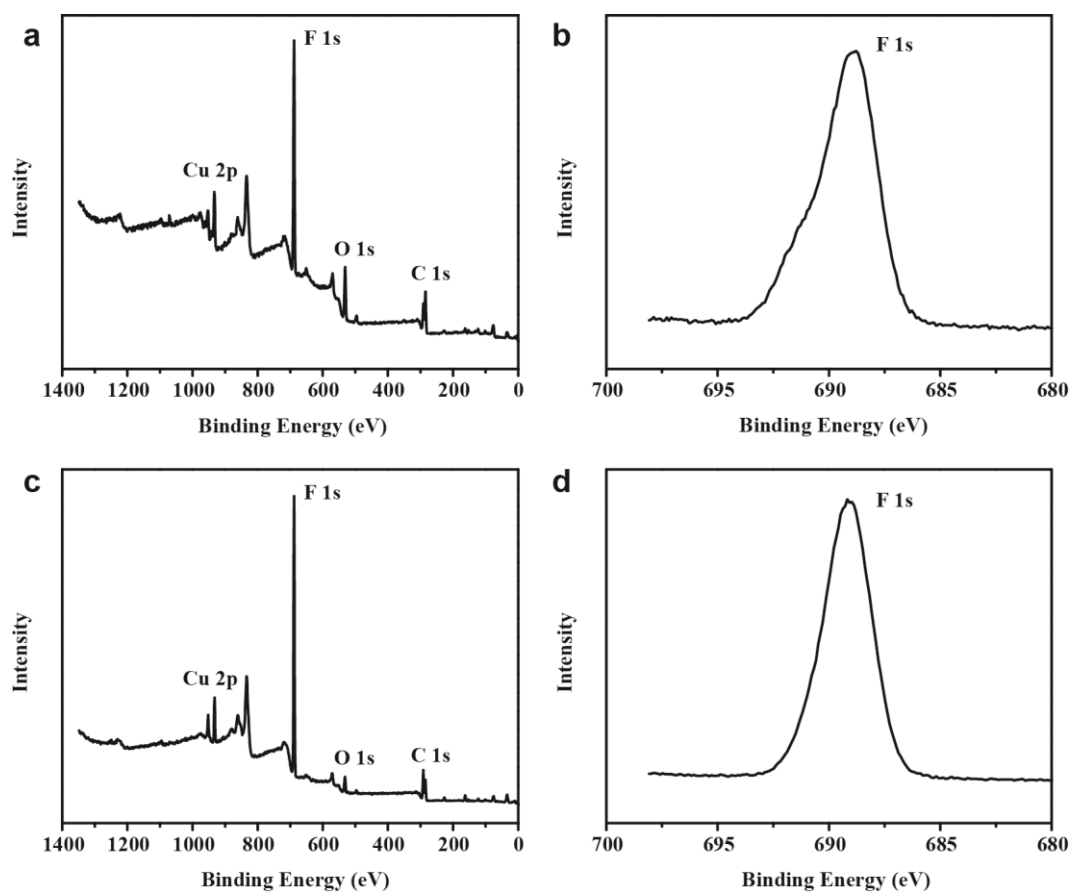


Figure S12. XPS spectra of the prepared fabrics modified with 0.2 mM (a, b) and 15 mM (c, d) 1H,1H,2H,2H-perfluorodecanethiol.

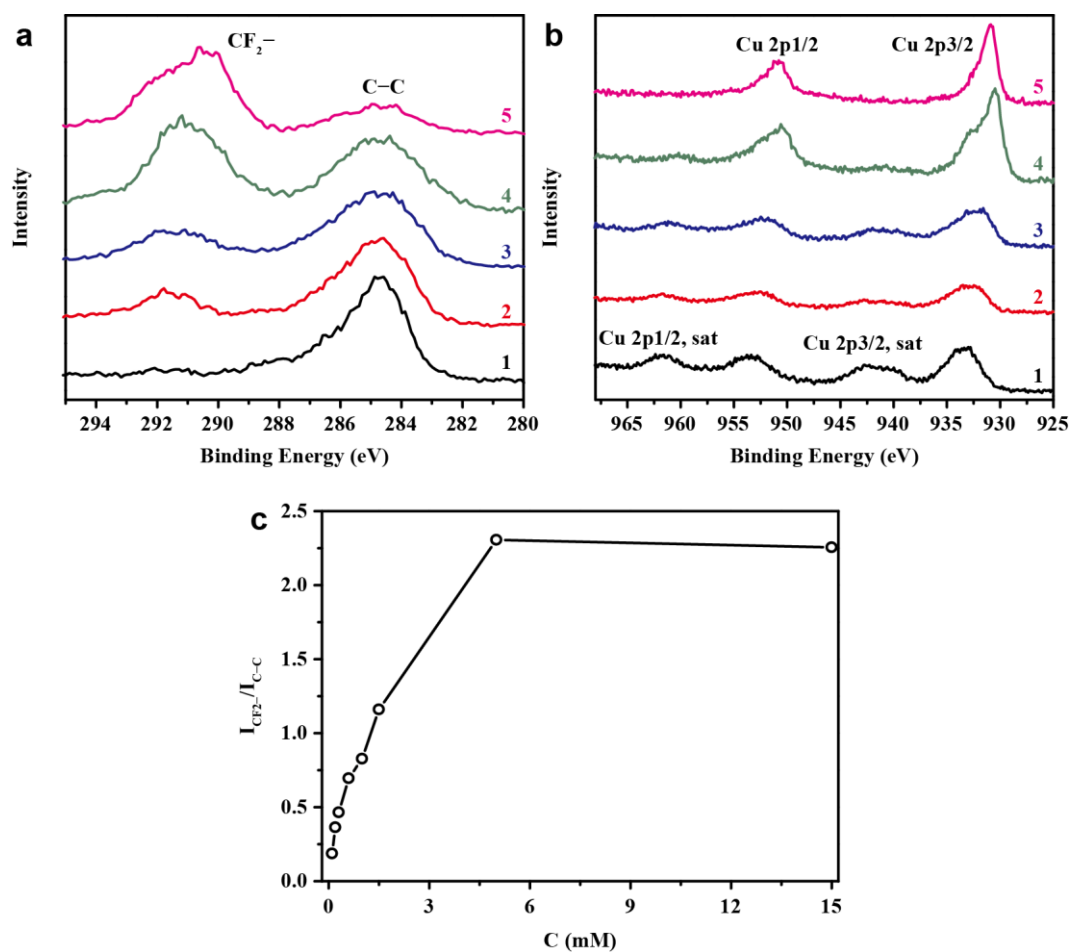


Figure S13. (a) C 1s and (b) Cu 2p XPS spectra of the CuO-coated fabrics after modification with 1H,1H,2H,2H-perfluorodecanethiol at different concentrations: (1) 0.1 mM, (2) 0.3 mM, (3) 1 mM, (4) 1.5 mM, and (5) 5 mM. (c) Intensity ratio of CF₂⁻ and C–C of the modified fabrics as a function of the thiol concentration.

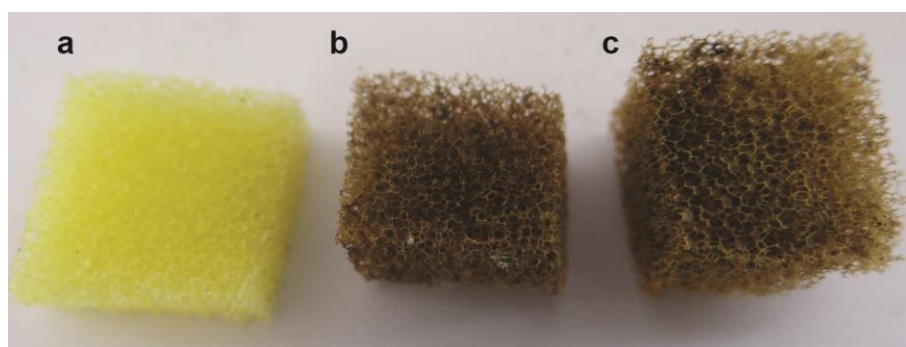


Figure S14. Photographs of original (a) and CuO-coated sponges before (b) and after (c) modification with 0.2 mM 1H,1H,2H,2H-perfluorodecanethiol.

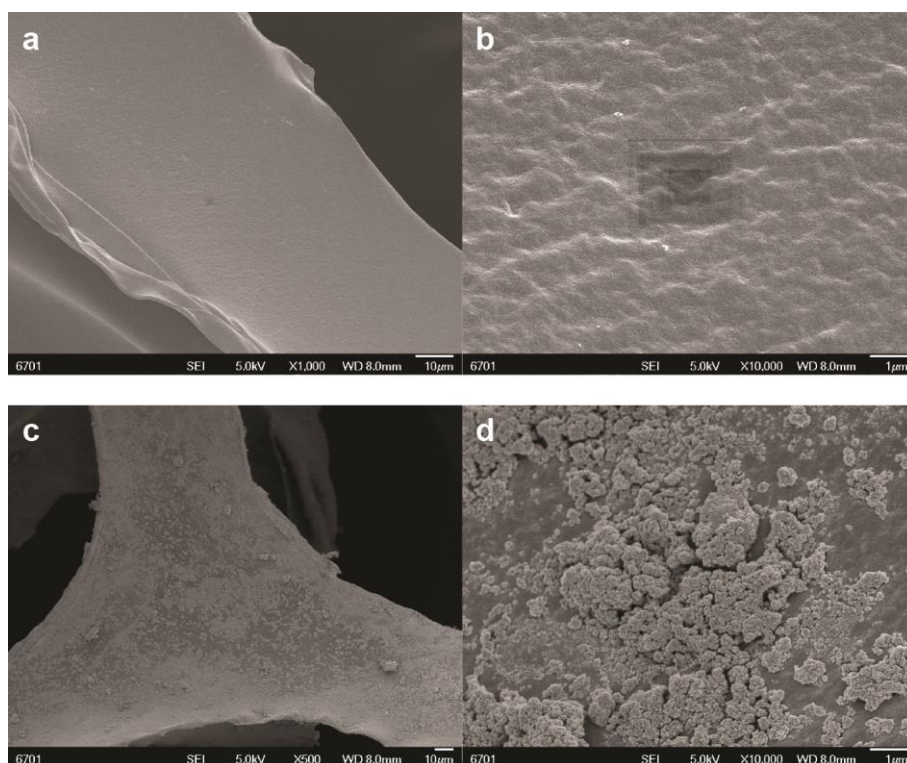


Figure S15. SEM images of original (a, b) and dual superlyophobic (c, d) sponges.

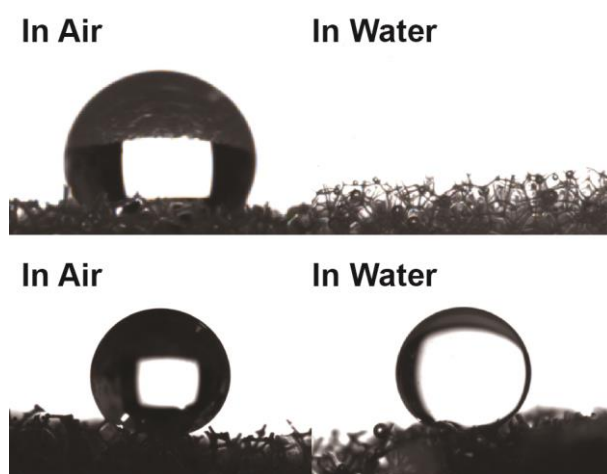


Figure S16. θ^*_w and θ^*_{ow} of original (upper) and dual superlyophobic (below) sponges.

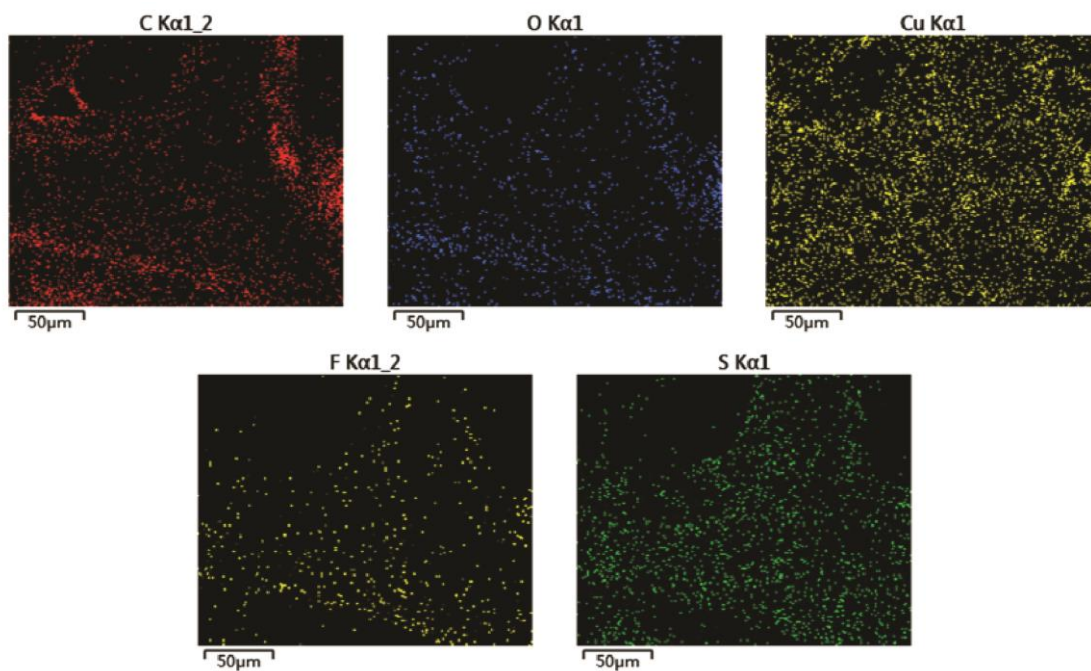


Figure S17. Element mapping images of dual superlyophobic sponge.

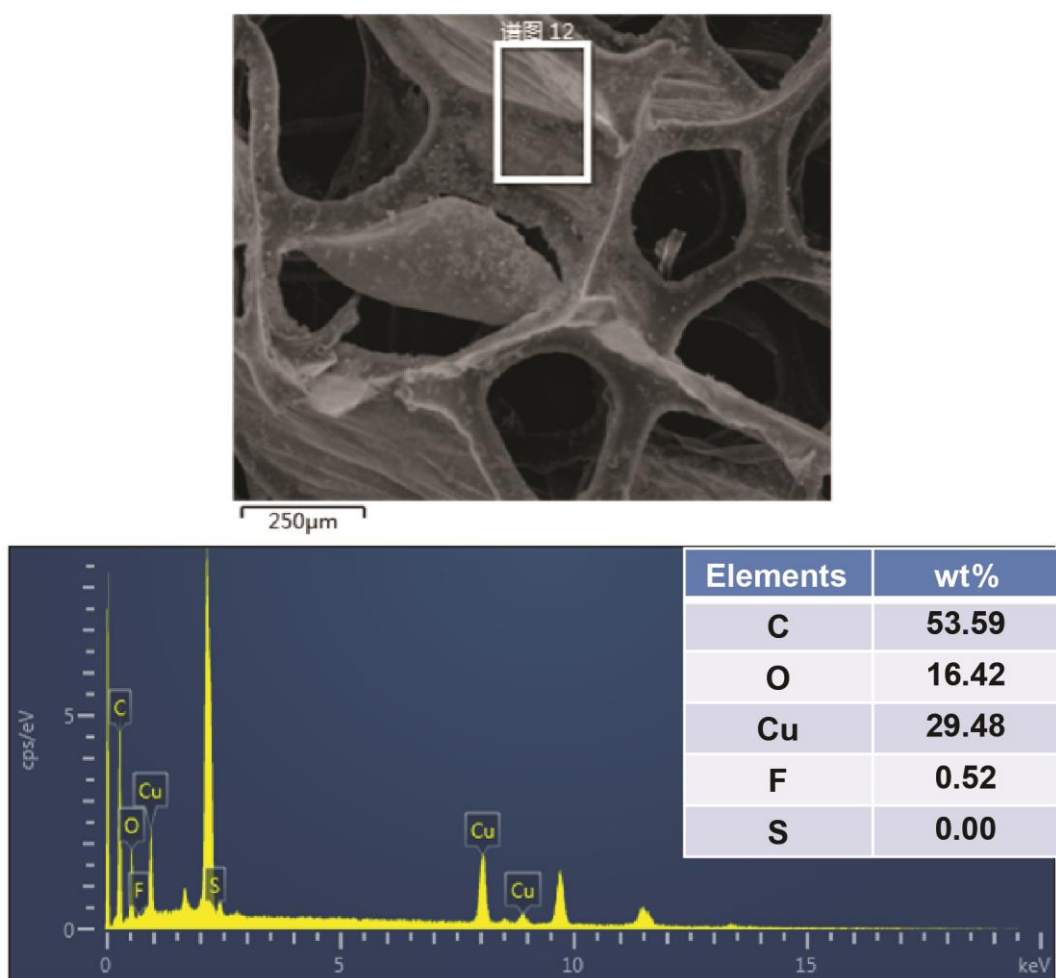


Figure S18. SEM image and element percent of dual superlyophobic sponge.

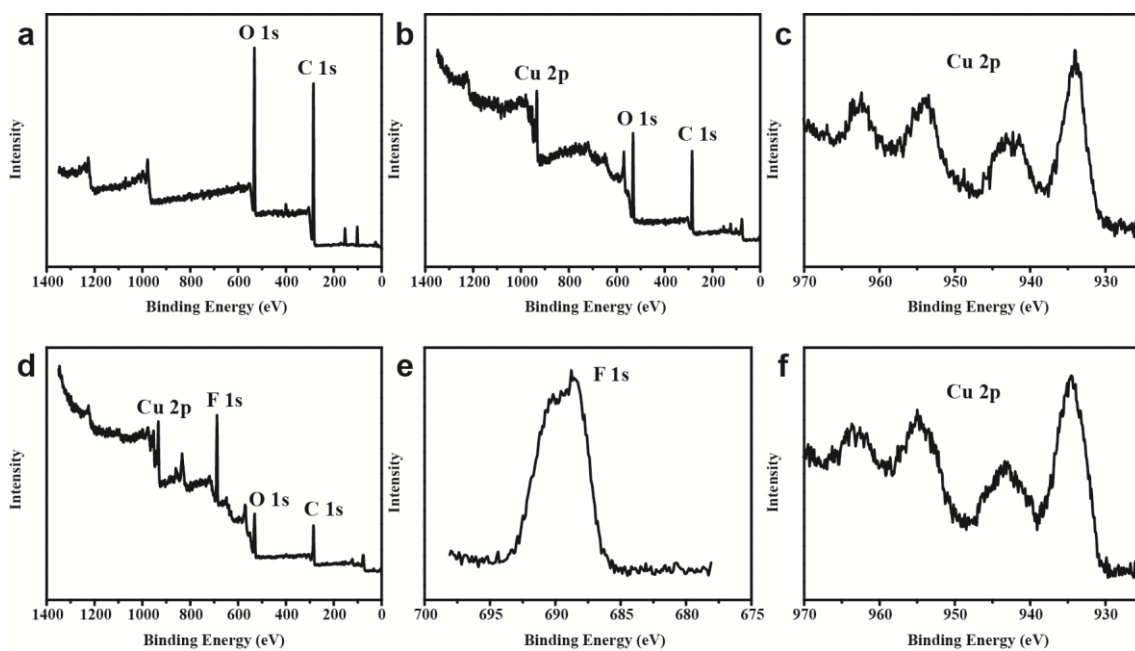


Figure S19. XPS spectra of original (a) and CuO-coated sponges before (b, c) and after (d-f) modification with 0.2 mM 1H,1H,2H,2H-perfluorodecanethiol.

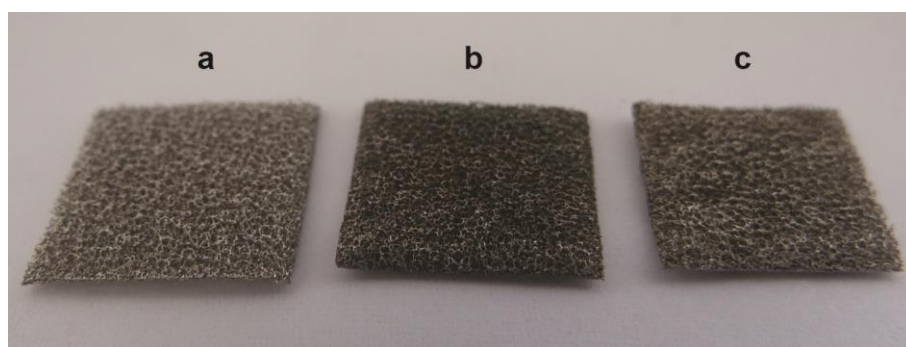


Figure S20. Photographs of original (a) and oxidized nickel foams before (b) and after (c) modification with 0.2 mM 1H,1H,2H,2H-perfluorodecanethiol.

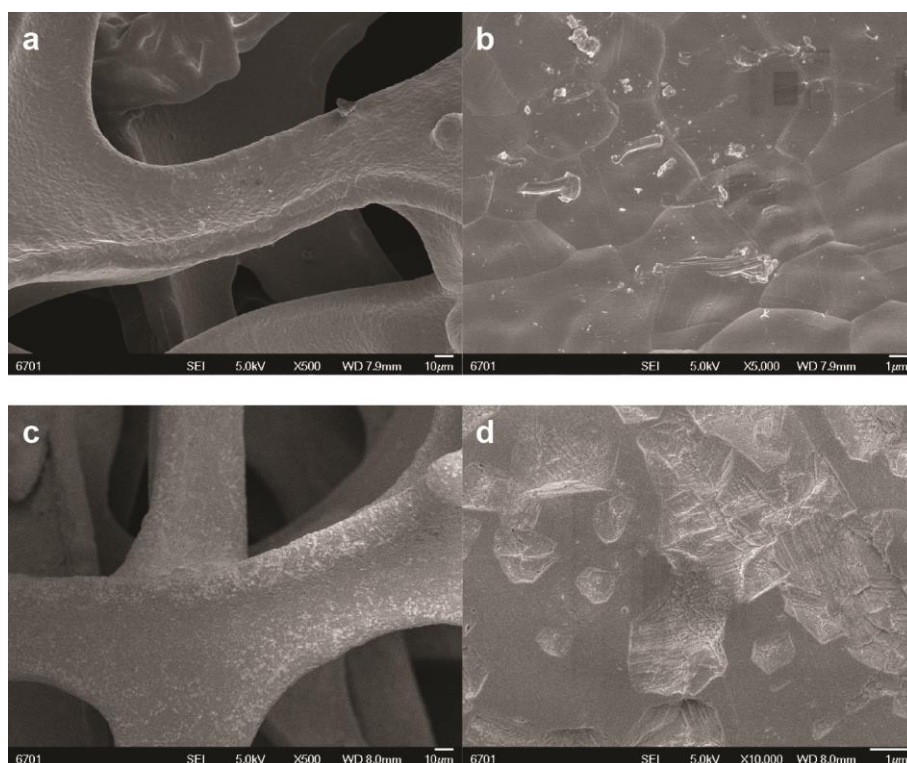


Figure S21. SEM images of original (a, b) and dual superlyophobic (c, d) nickel foams.

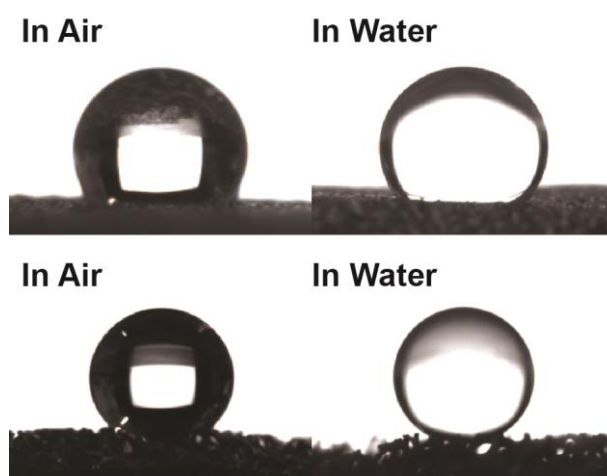


Figure S22. θ^*_w and θ^*_{ow} of original (upper) and dual superlyophobic (below) nickel foams.

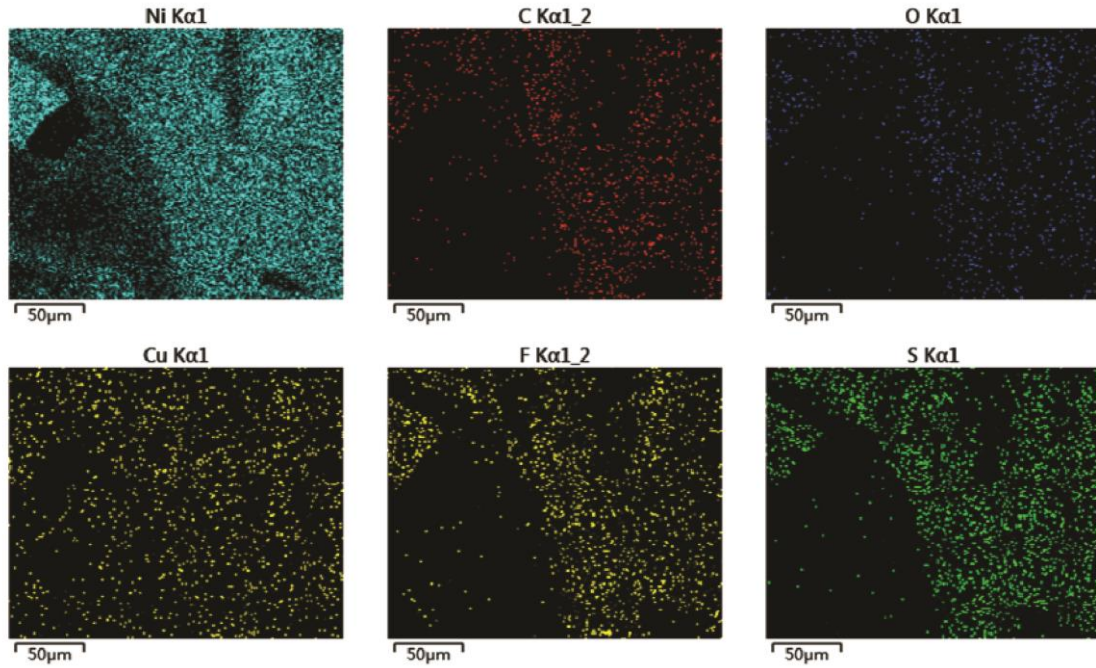


Figure S23. Element mapping images of dual superlyophobic nickel foam.

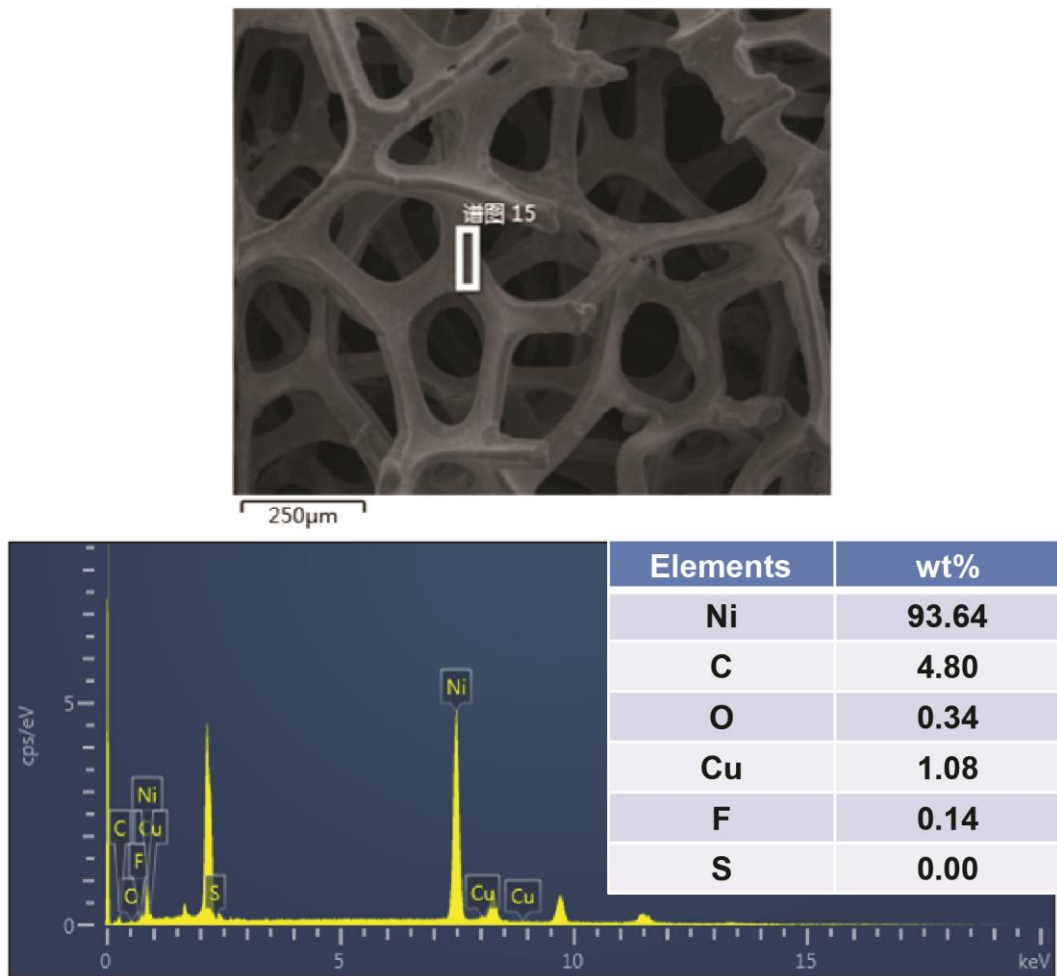


Figure S24. SEM image and element percent of dual superlyophobic nickel foam.

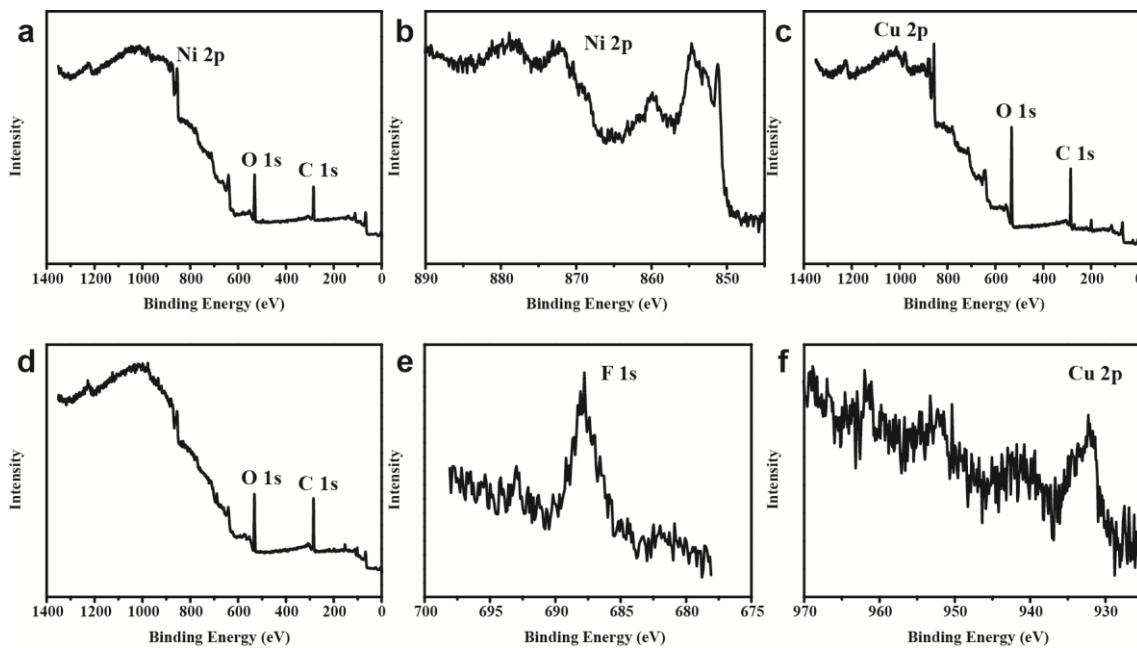


Figure S25. XPS spectra of original (a, b) and oxidized nickel foams before (c) and after (d-f) modification with 0.2 mM 1H,1H,2H,2H-perfluorodecanethiol.

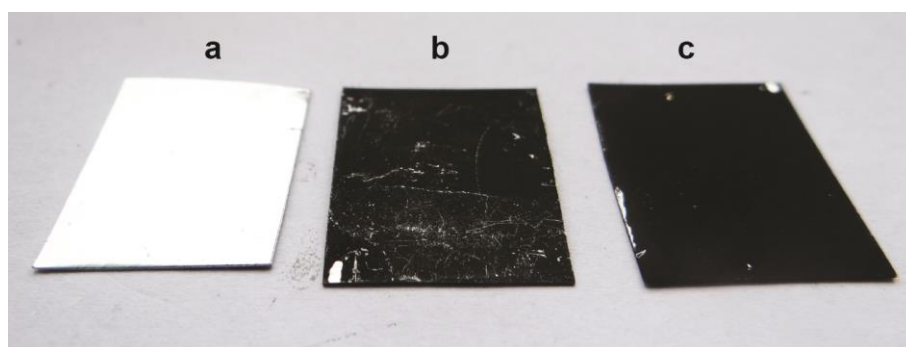


Figure S26. Photographs of original (a) and oxidized zinc sheets before (b) and after (c) modification with 0.2 mM 1H,1H,2H,2H-perfluorodecanethiol.

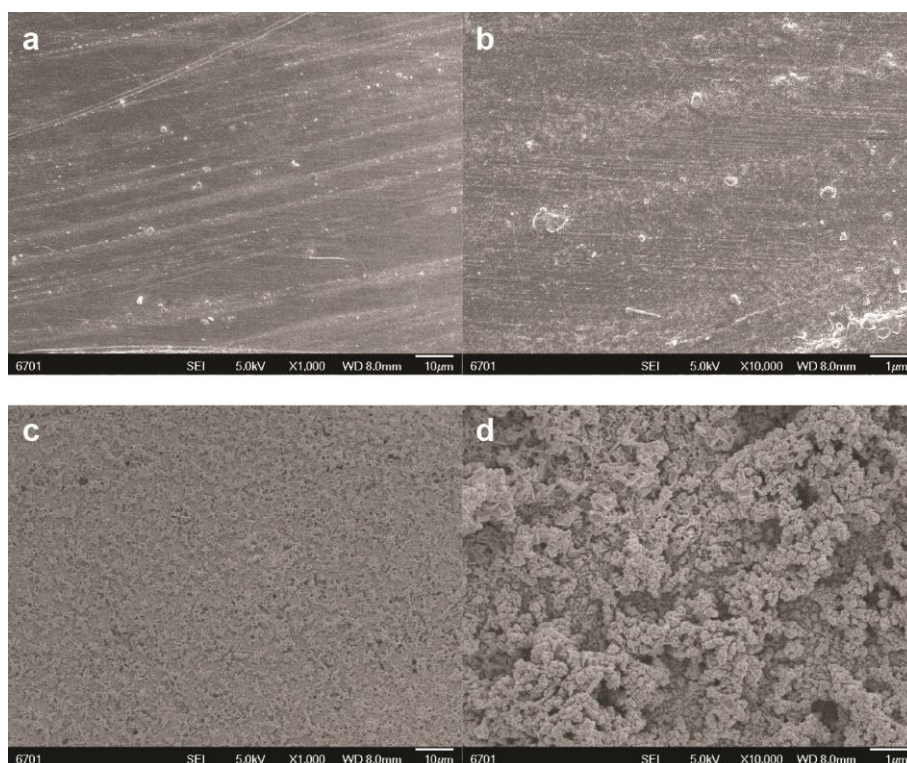


Figure S27. SEM images of original (a, b) and dual superlyophobic (c, d) zinc sheets.

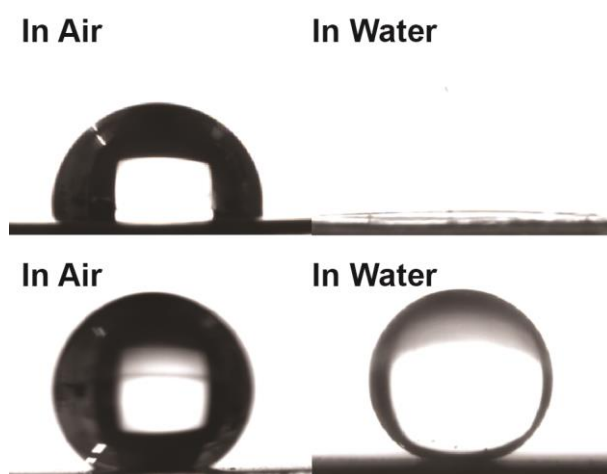


Figure S28. θ^*_{w} and θ^*_{ow} of original (upper) and dual superlyophobic (below) zinc sheets.

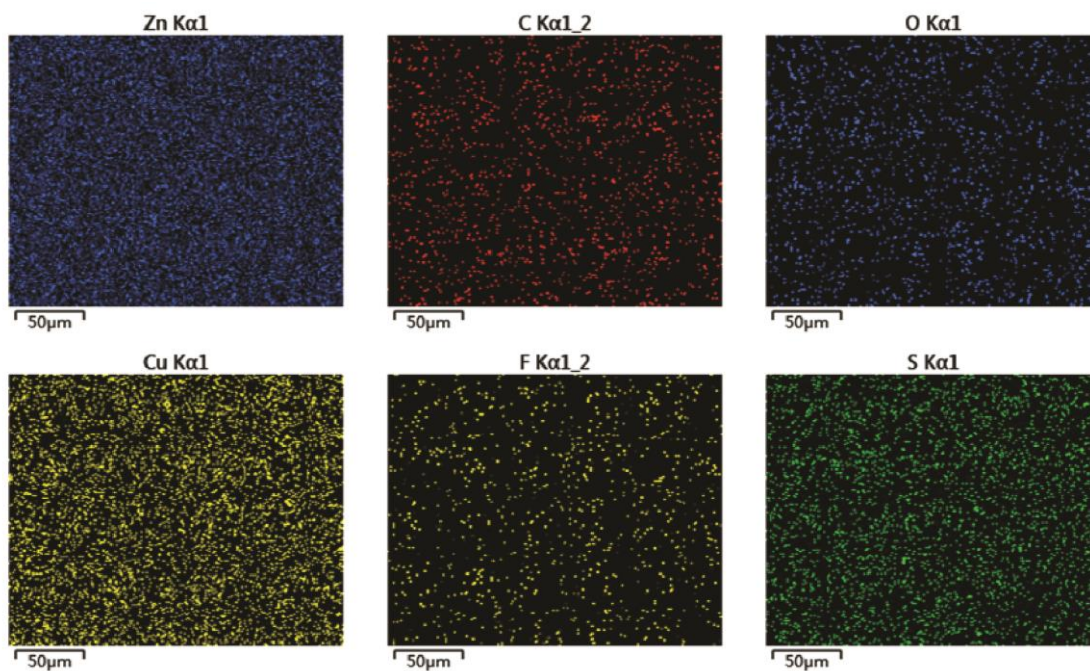


Figure S29. Element mapping images of dual superlyophobic zinc sheet.

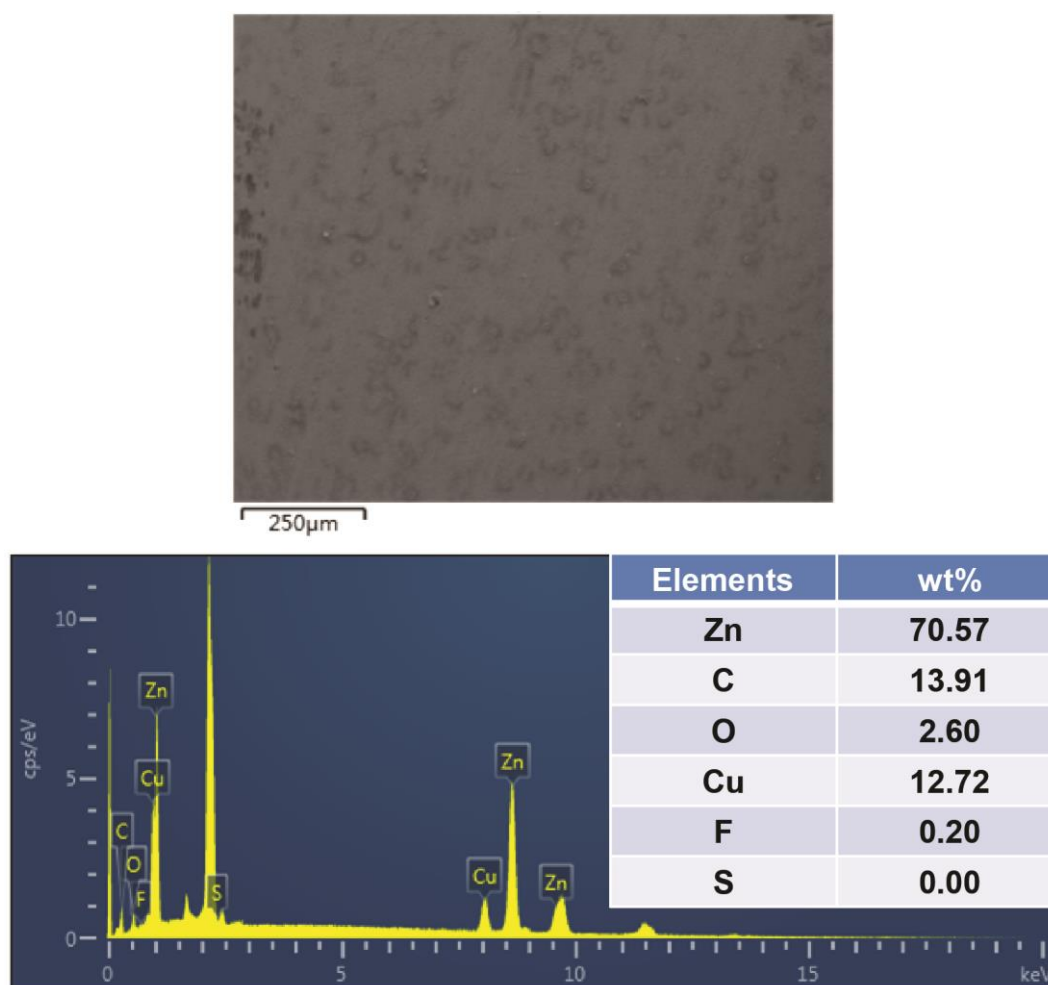


Figure S30. SEM image and element percent of dual superlyophobic zinc sheet.

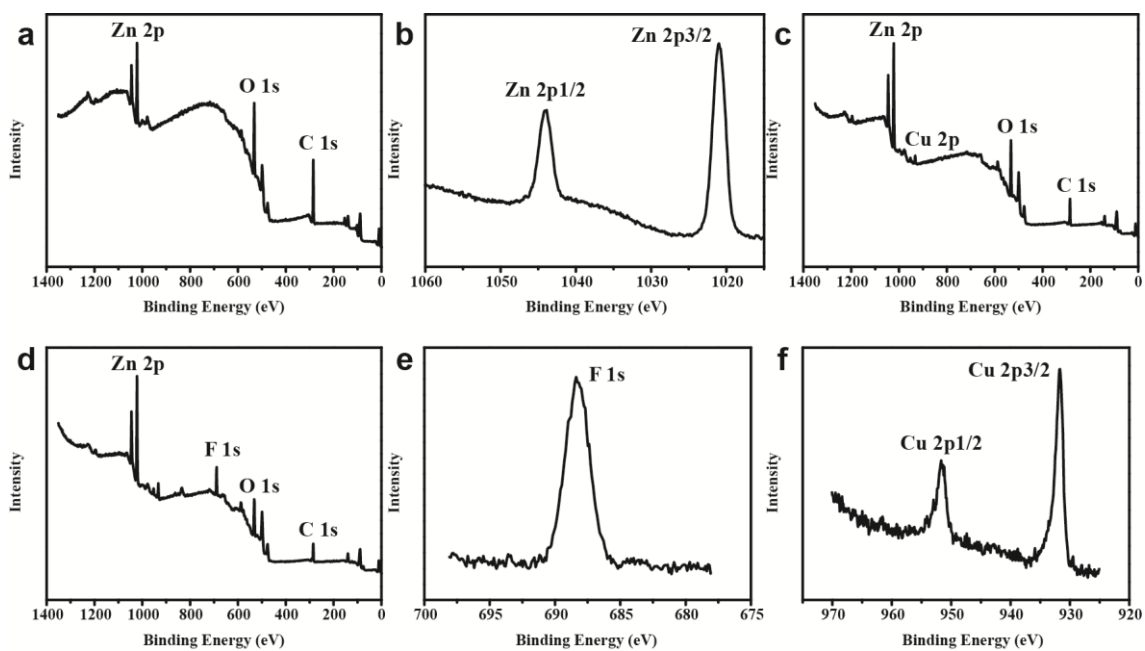


Figure S31. XPS spectra of original (a, b) and oxidized zinc sheets before (c) and after (d-f) modification with 0.2 mM 1H,1H,2H,2H-perfluorodecanethiol.

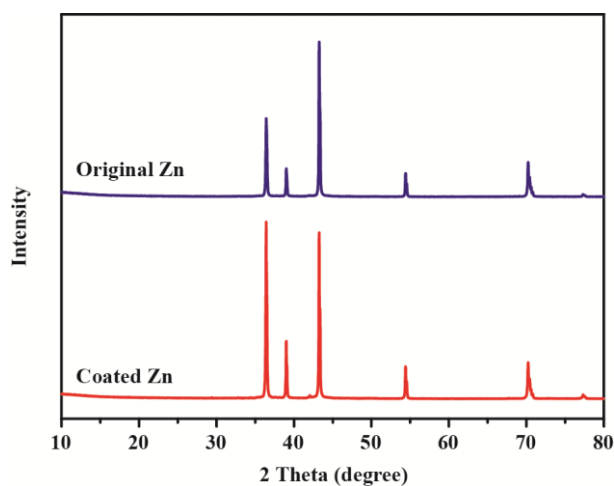


Figure S32. XRD patterns of original and dual superlyophobic zinc sheets.

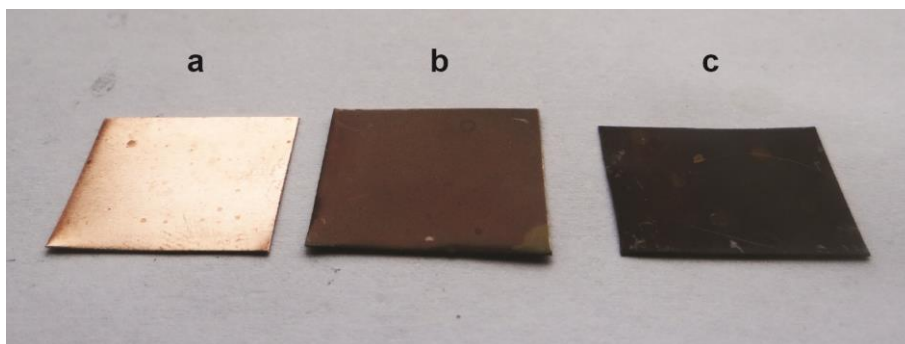


Figure S33. Photographs of original (a) and oxidized copper sheets before (b) and after (c) modification with 0.2 mM 1H,1H,2H,2H-perfluorodecanethiol.

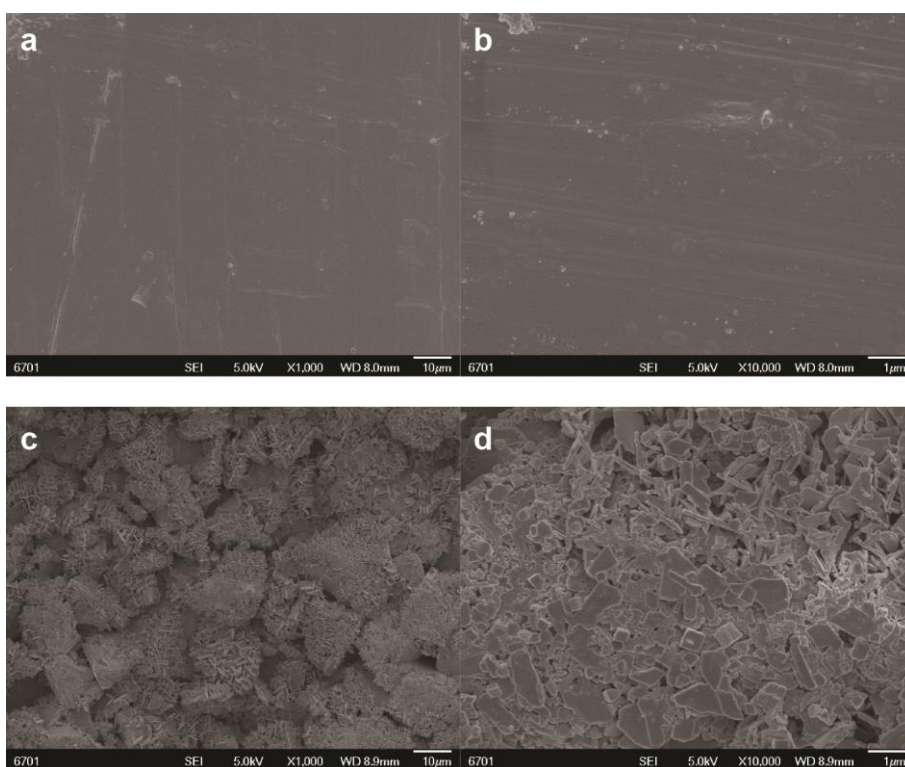


Figure S34. SEM images of original (a, b) and dual superlyophobic (c, d) copper sheets.

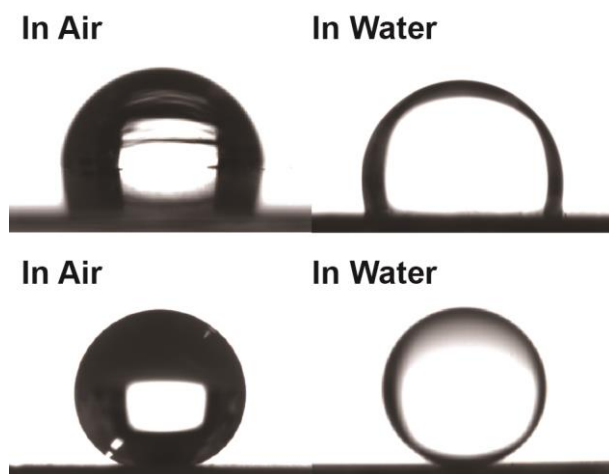


Figure S35. θ^*_{w} and θ^*_{ow} of original (upper) and dual superlyophobic (below) copper sheets.

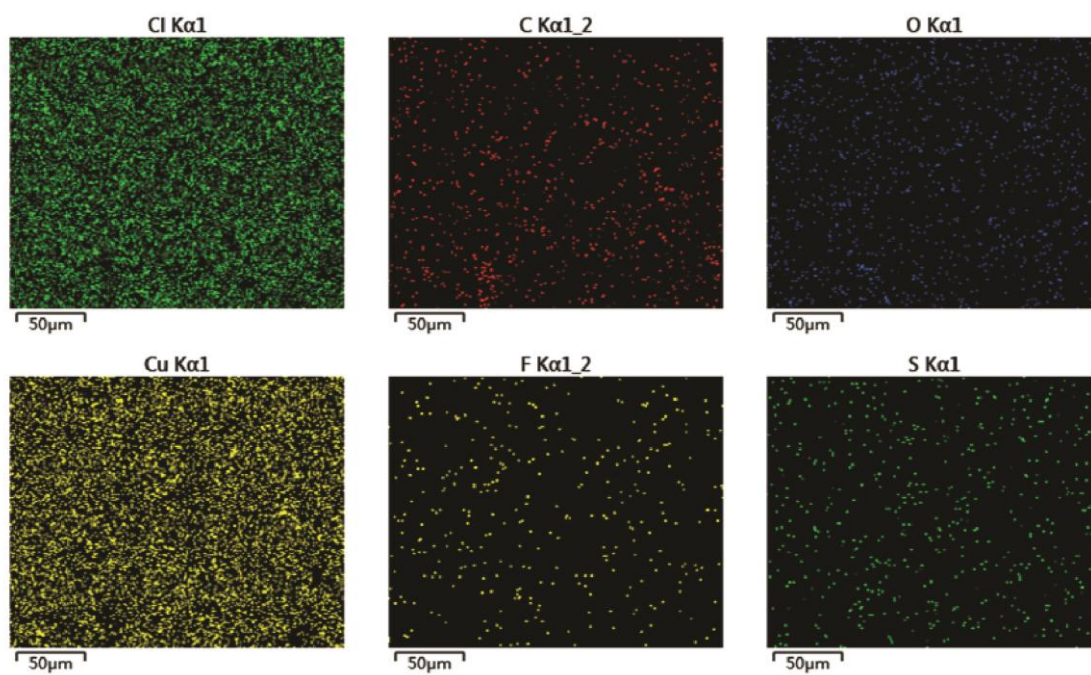


Figure S36. Element mapping images of dual superlyophobic copper sheet.

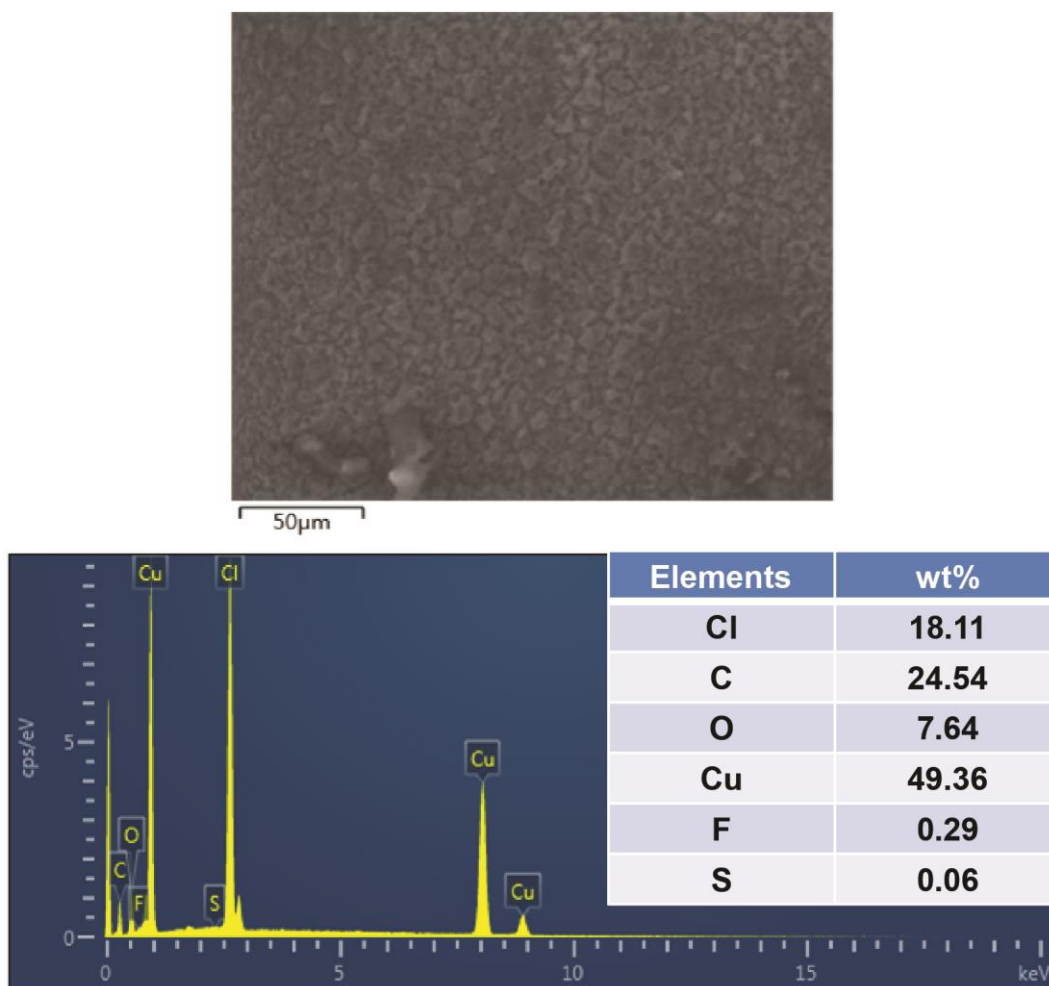


Figure S37. SEM image and element percent of dual superlyophobic copper sheet.

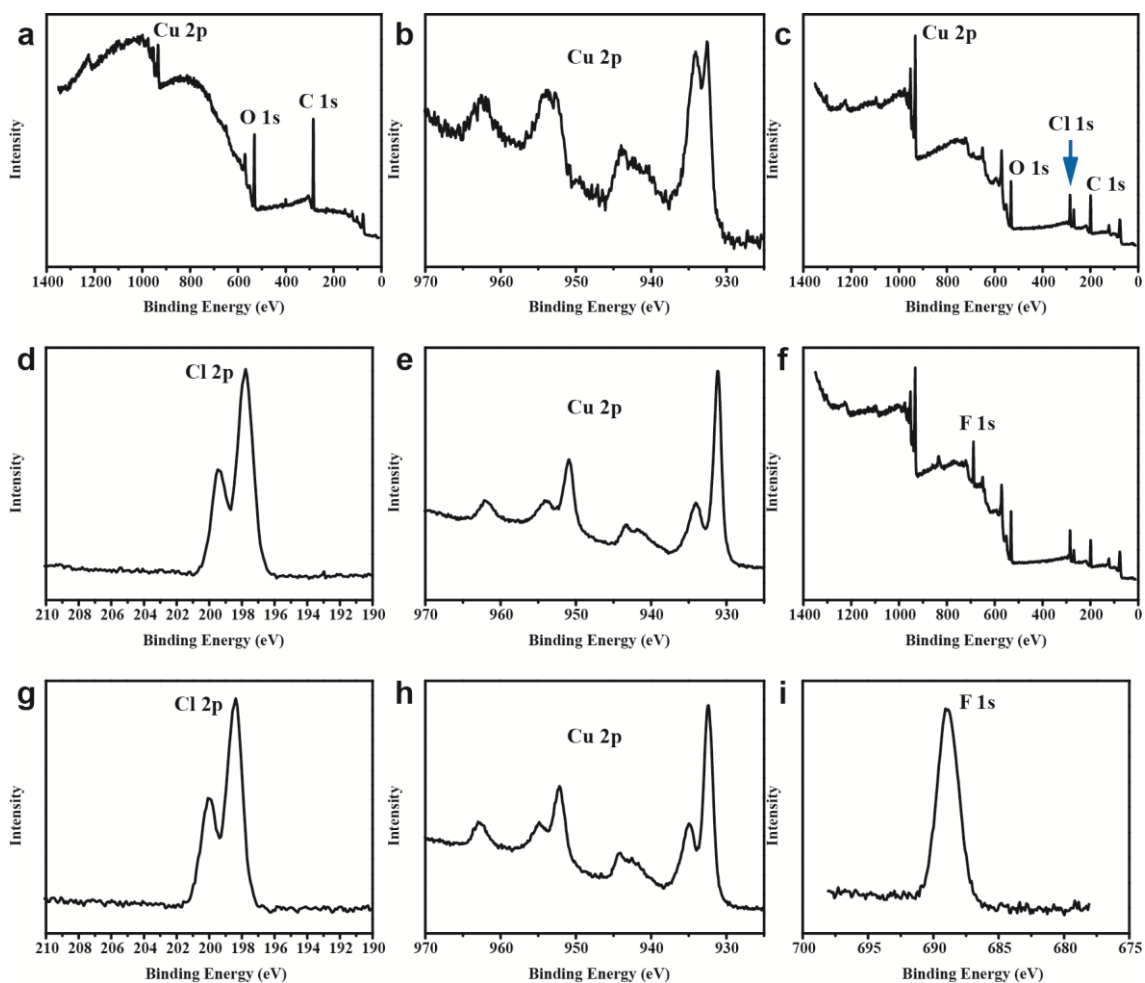


Figure S38. XPS spectra of original (a, b), oxidized (c-e), and dual superlyophobic (f-i) copper sheets.

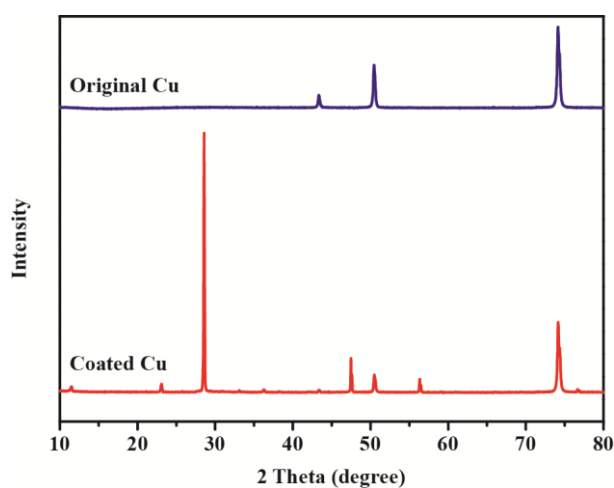


Figure S39. XRD patterns of original and dual superlyophobic copper sheets.

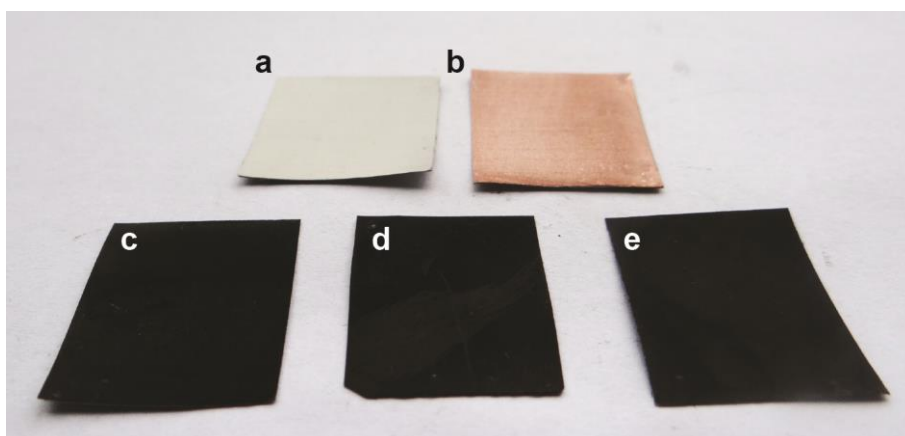


Figure S40. Photographs of original (a), Cu-coated (b), oxidized (c), heat-treated (d), and dual superlyophobic (e) SSMs.

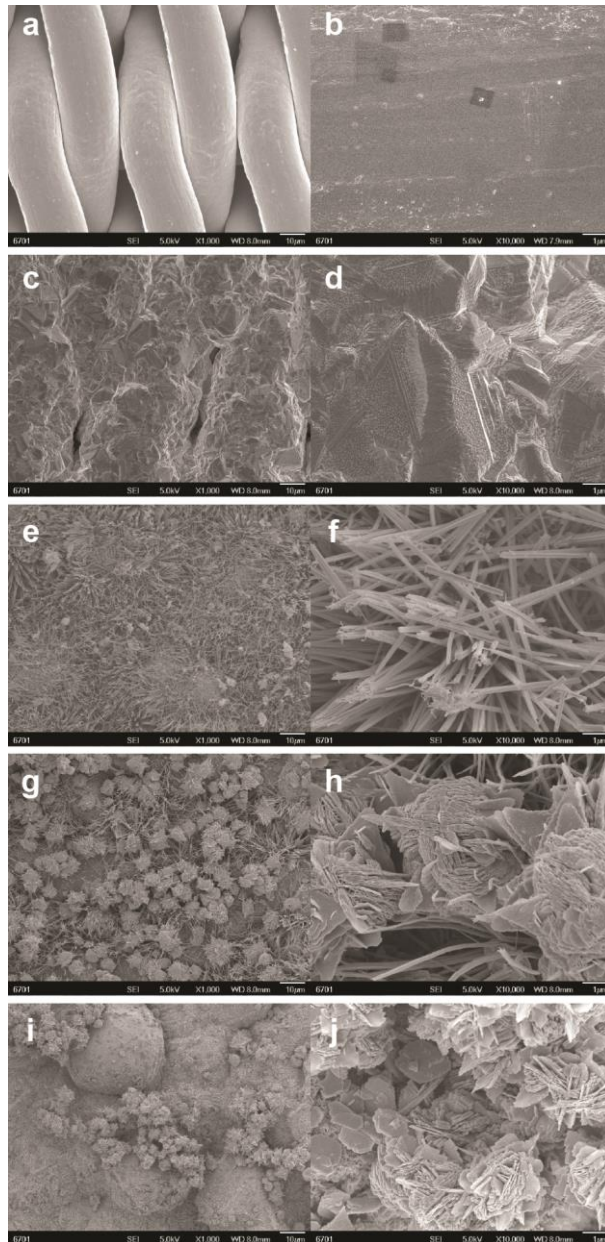


Figure S41. SEM images of original (a, b), Cu-coated (c, d), oxidized (e, f), heat-treated (g, h), and dual superlyophobic (i, j) SSMSs.

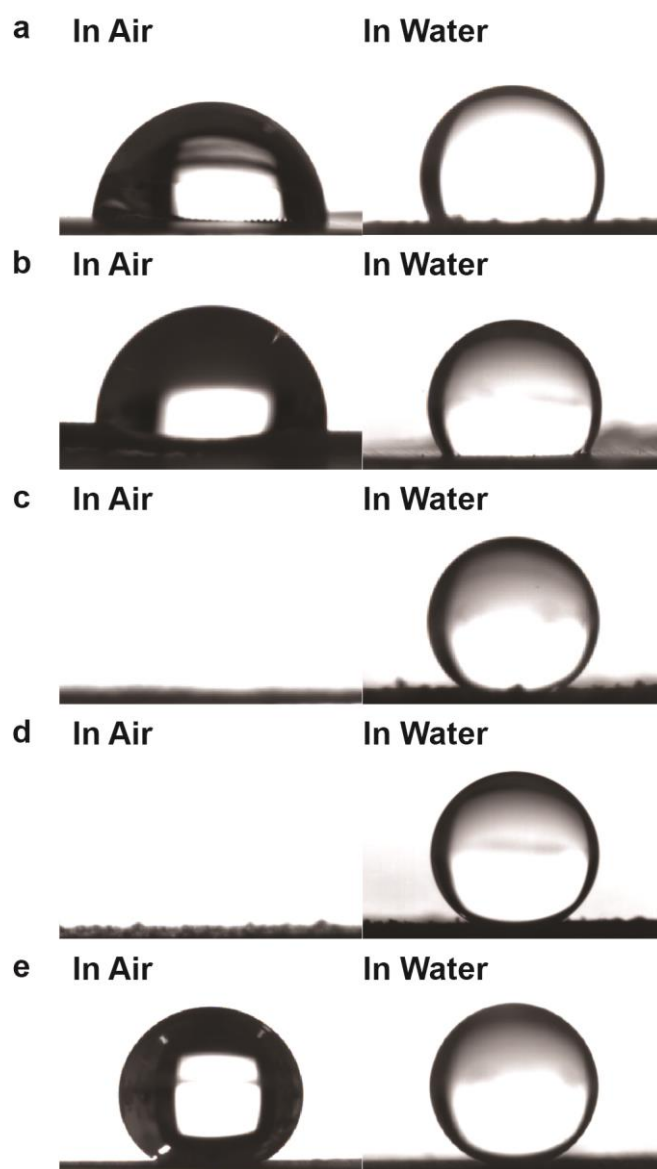


Figure S42. θ^*_w and θ^*_{ow} of original (a), Cu-coated (b), oxidized (c), heat-treated (d), and dual superlyophobic (e) SSMs.

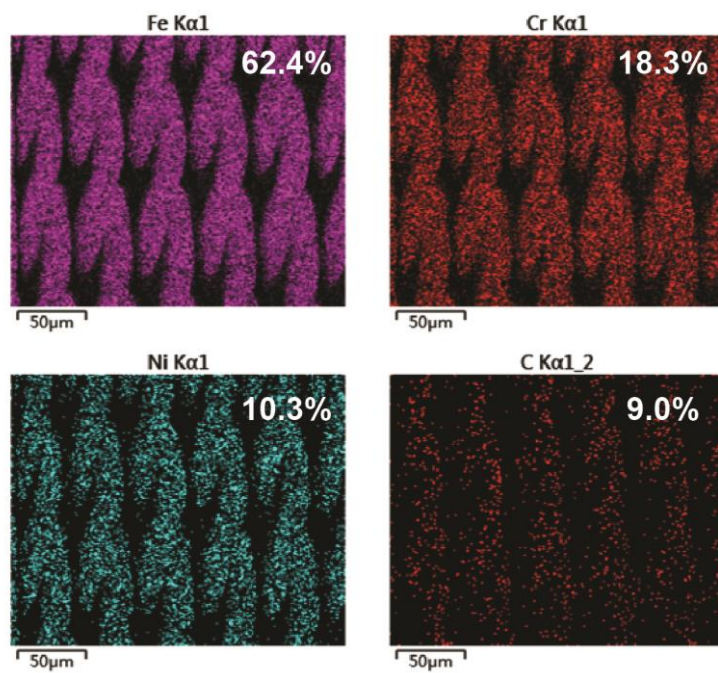


Figure S43. Element mapping images and element percent of original SSM.

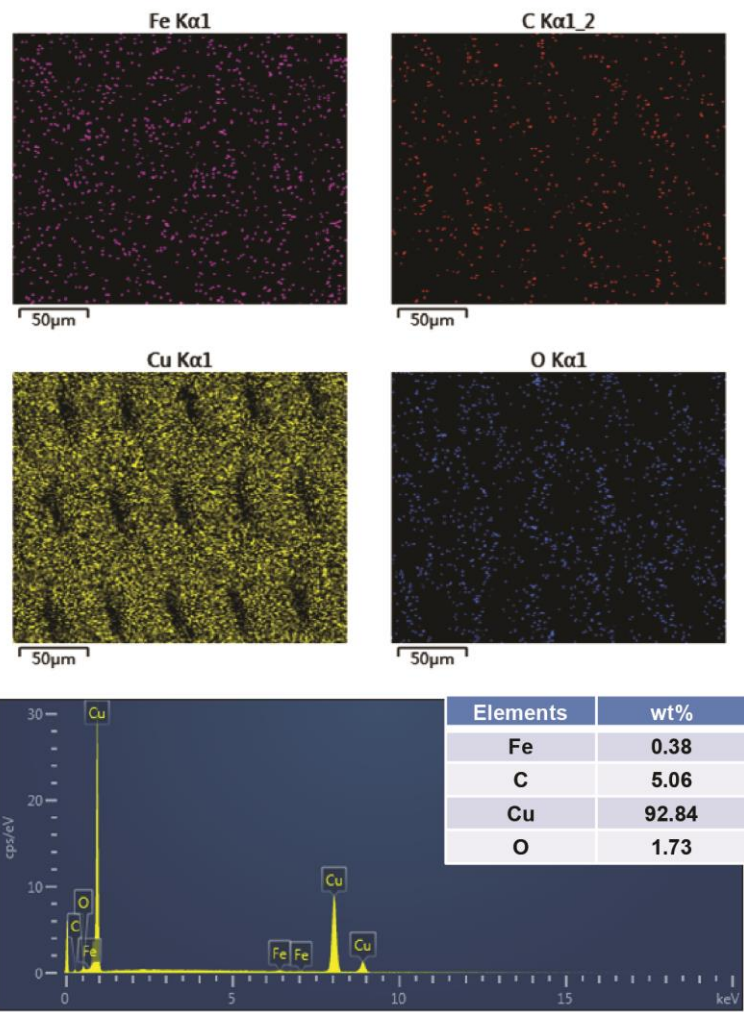


Figure S44. Element mapping images and element percent of Cu-coated SSM.

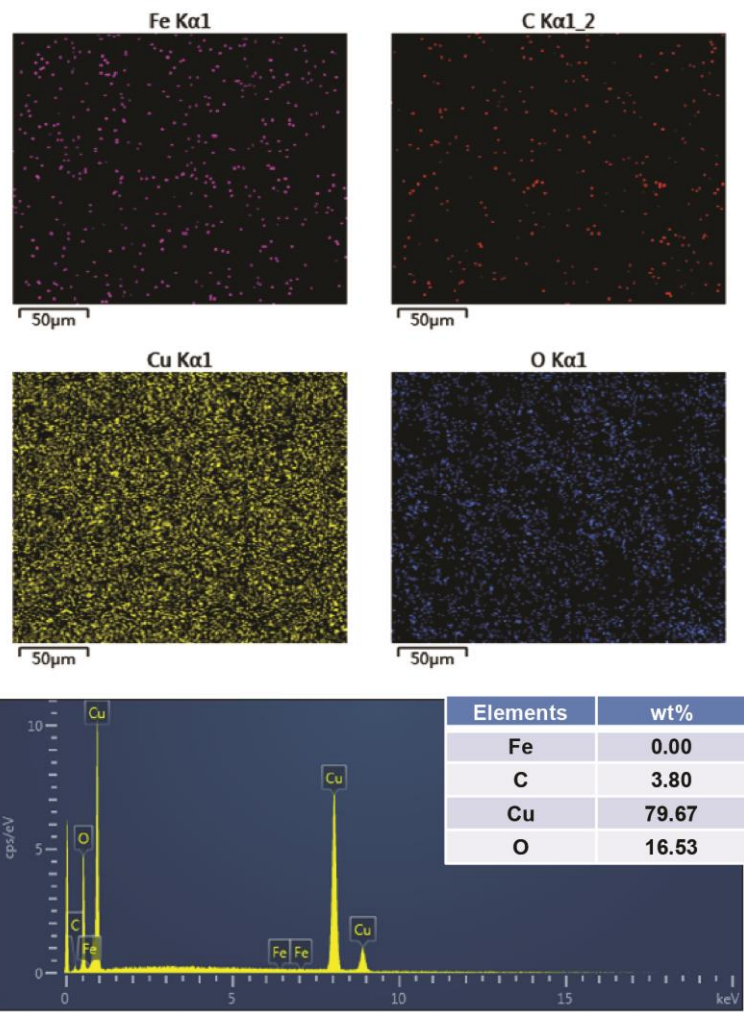


Figure S45. Element mapping images and element percent of oxidized SSM.

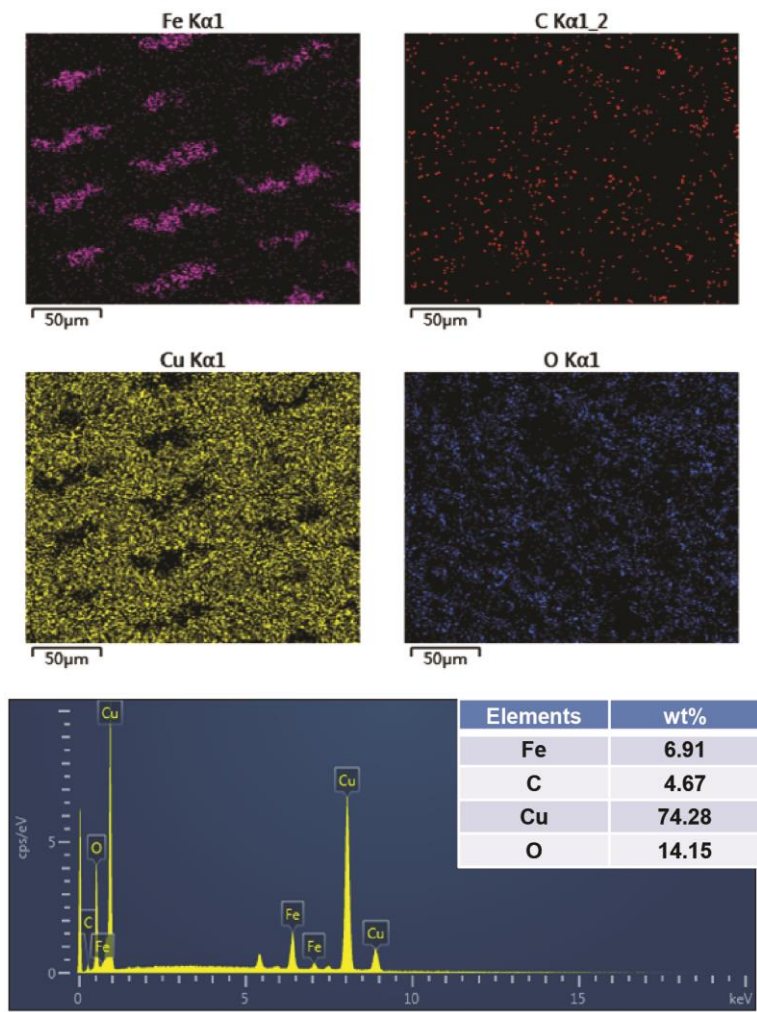


Figure S46. Element mapping images and element percent of heat-treated SSM.

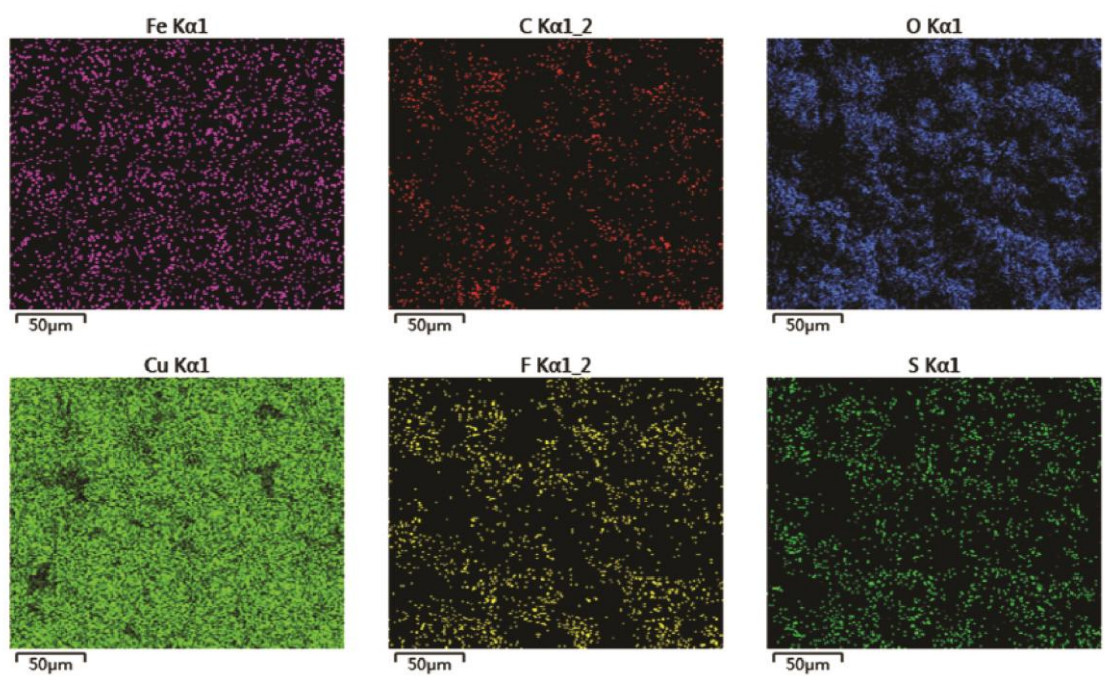


Figure S47. Element mapping images of dual superlyophobic SSM.

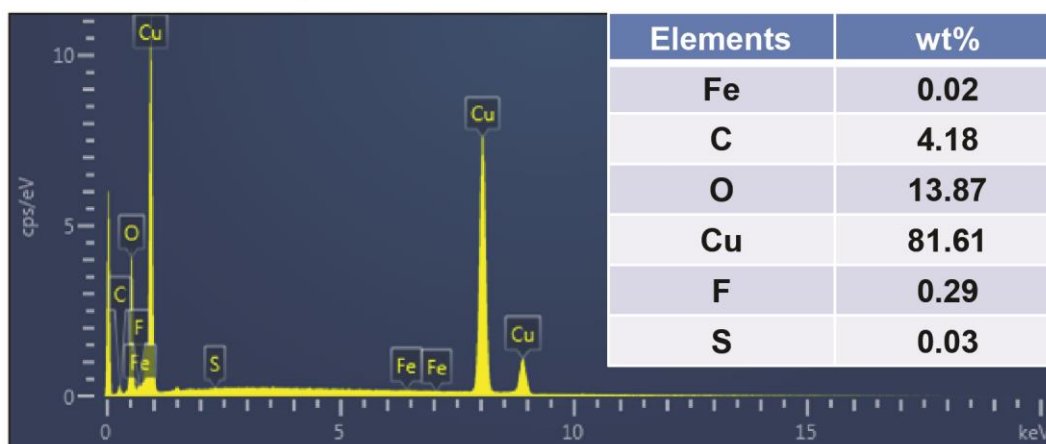
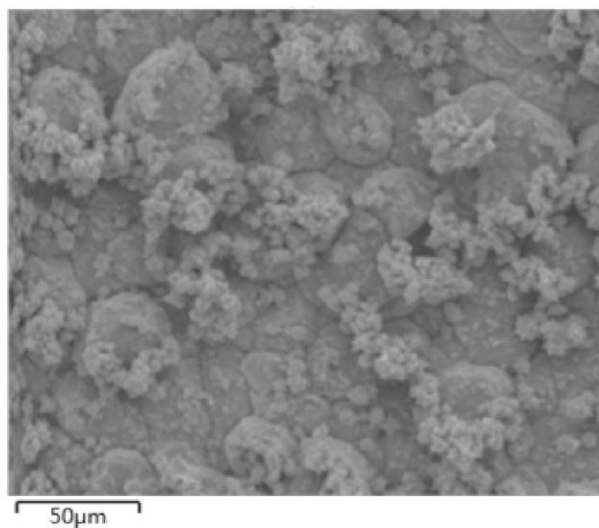


Figure S48. SEM image and element percent of dual superlyophobic SSM.

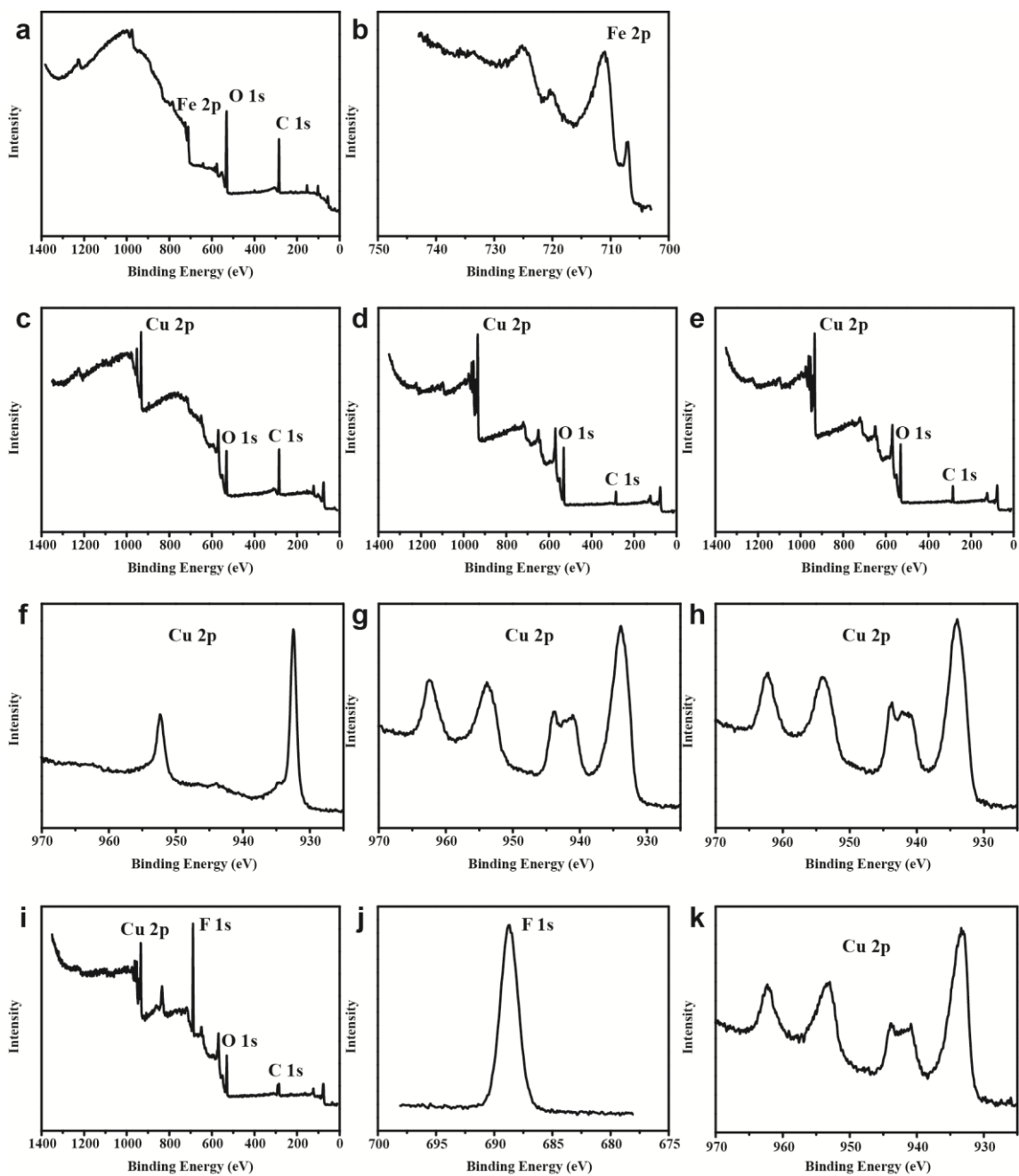


Figure S49. XPS spectra of original (a, b), Cu-coated (c, f), oxidized (d, g), heat-treated (e, h), and dual superlyophobic (i-k) SSMs.

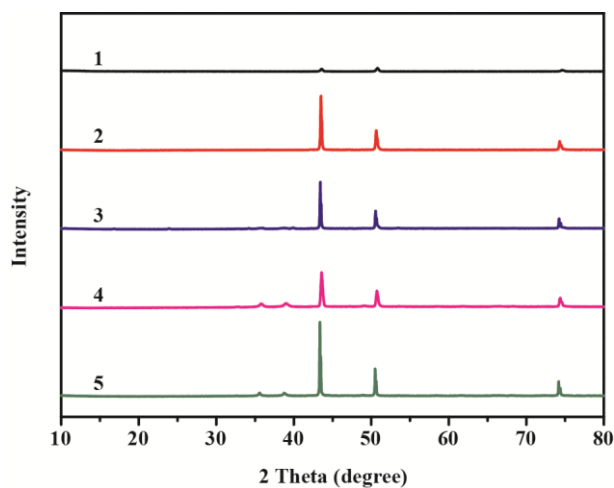


Figure S50. XRD patterns of original (1), Cu-coated (2), oxidized (3), heat-treated (4), and dual superlyophobic (5) SSMs.

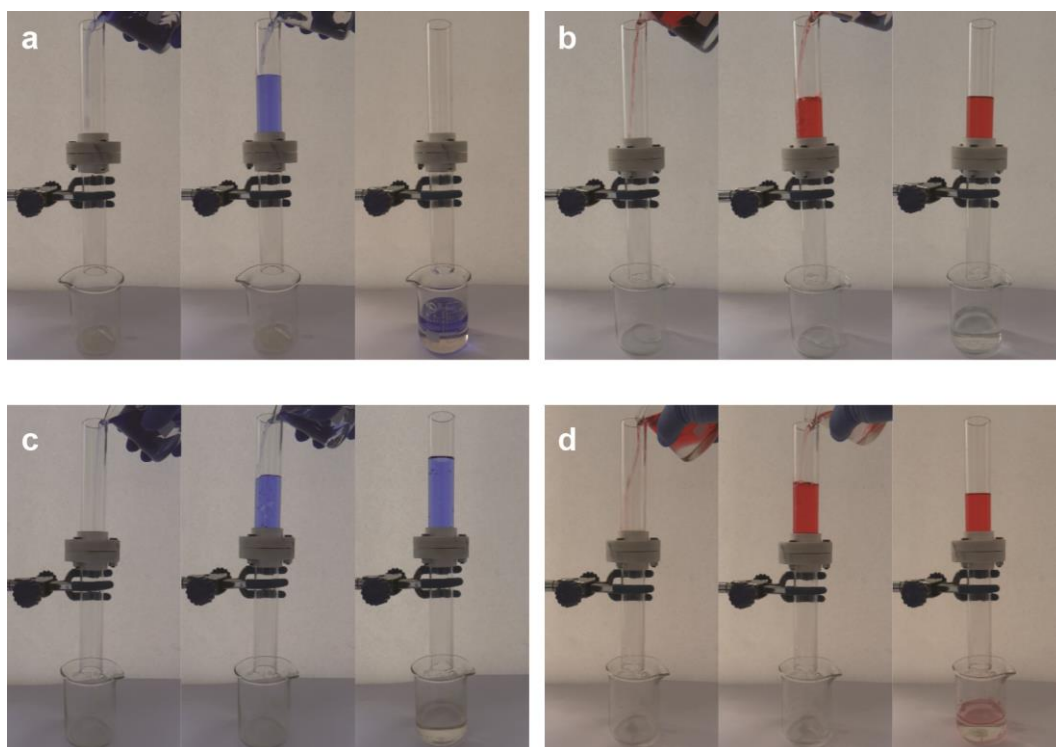


Figure S51. (a) Dichloroethane-water and (b) hexane-water mixtures are separated by the superhydrophilic fabric with the CuO coating. (c) Dichloroethane-water and (d) hexane-water mixtures are separated by the superhydrophobic fabric modified with 15 mM 1H,1H,2H,2H-perfluorodecanethiol. Water in (a, c) and hexane in (b, d) are dyed by methylene blue and Sudan red, respectively.

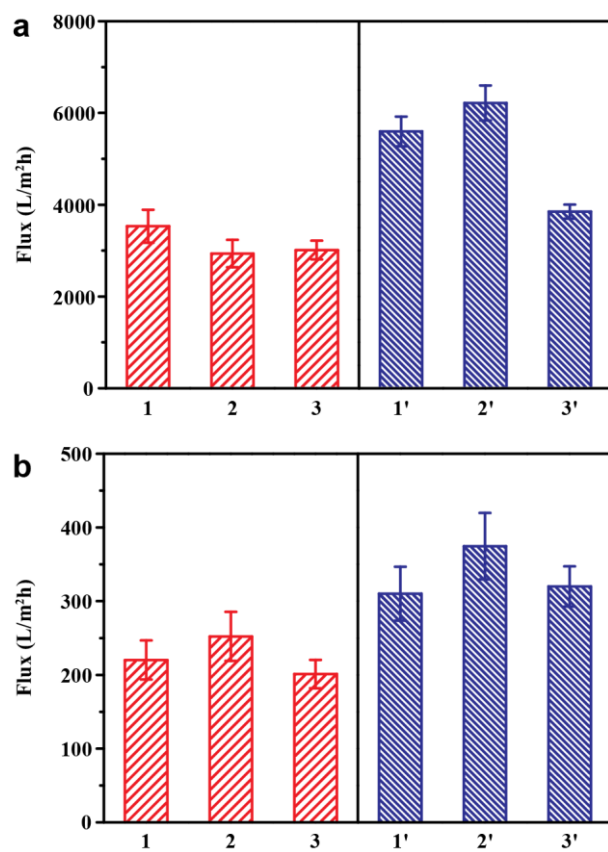


Figure S52. Flux of immiscible oil-water mixtures (a) and emulsions (b) during separation using the dual superlyophobic fabric (a) and SSM (b), respectively. Oils include hexane (1), toluene (2), diesel (3, 3'), chloroform (1'), and 1,2-dichloroethane (2').

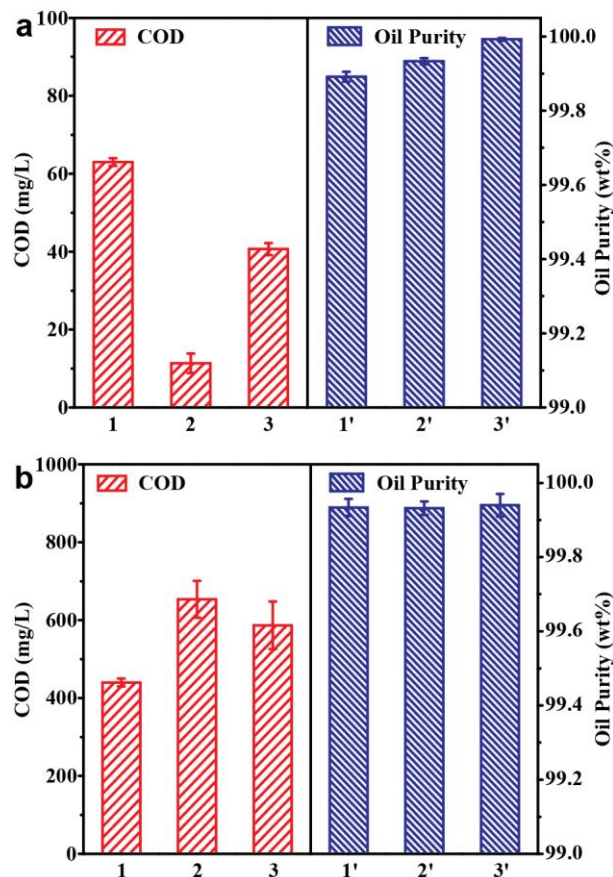


Figure S53. COD and oil purity in collected filtrates of immiscible oil-water mixtures (a) and emulsions (b) after separation using the dual superlyophobic fabric (a) and SSM (b), respectively. Oils include hexane (1), toluene (2), diesel (3, 3'), chloroform (1'), and 1,2-dichloroethane (2').



Figure S54. Photographs of hexane-in-water (a) and toluene-in-water (b) emulsions before (left) and after (right) separation using the dual superlyophobic SSM.

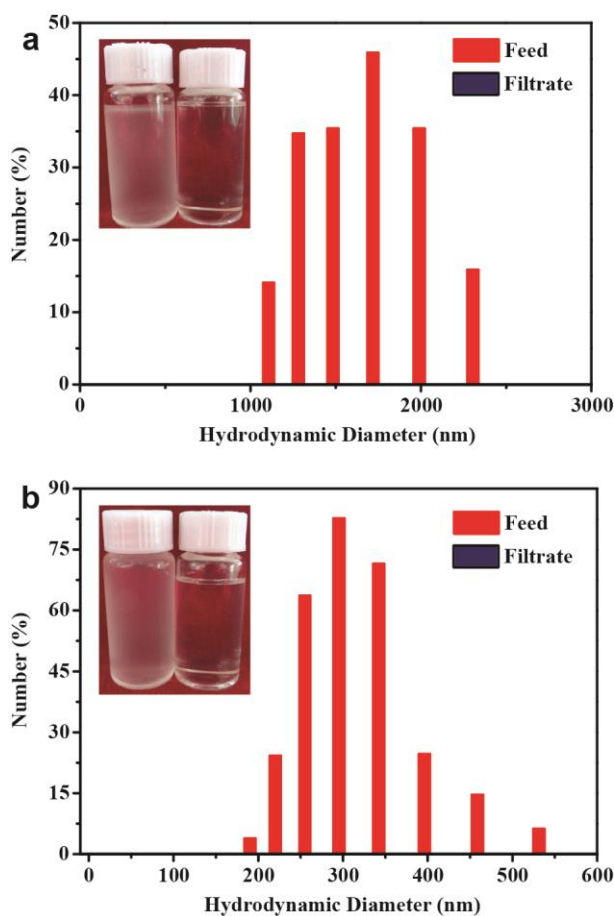


Figure S55. DLS and photographs (insets) of water-in-chloroform (a) and water-in-dichloroethane (b) emulsions before (left) and after (right) separation using the dual superlyophobic SSM.

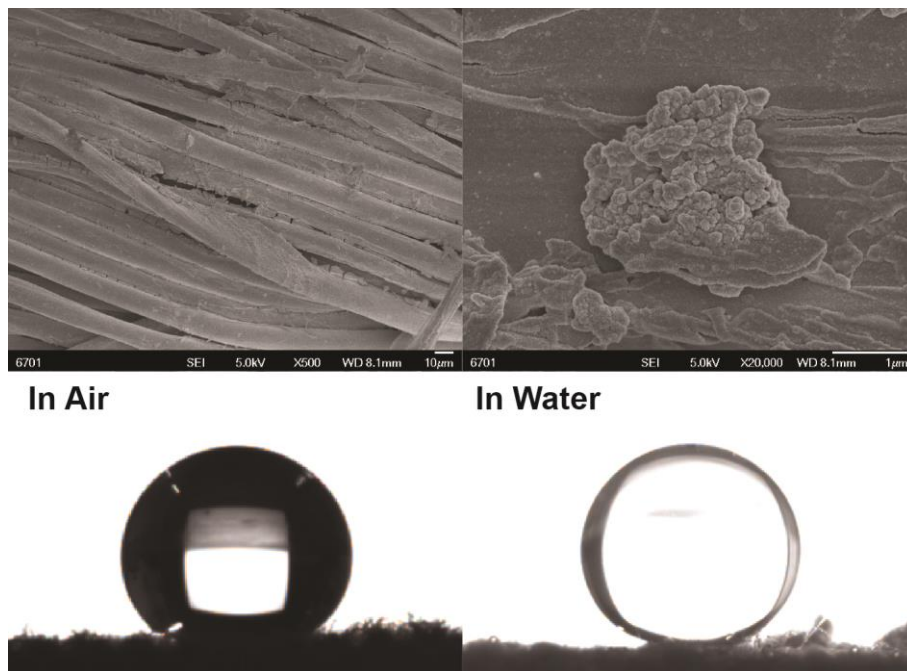


Figure S56. SEM images, θ^*_w and θ^*_{ow} of the dual superlyophobic fabric after 10 separation cycles.

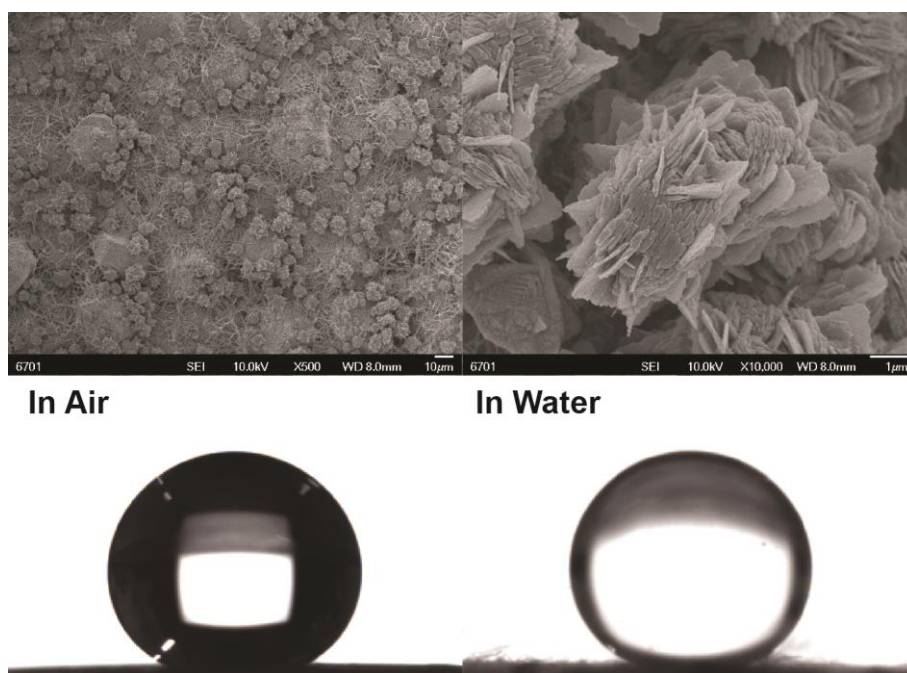


Figure S57. SEM images, θ^*_w and θ^*_{ow} of the dual superlyophobic SSM after 10 separation cycles.

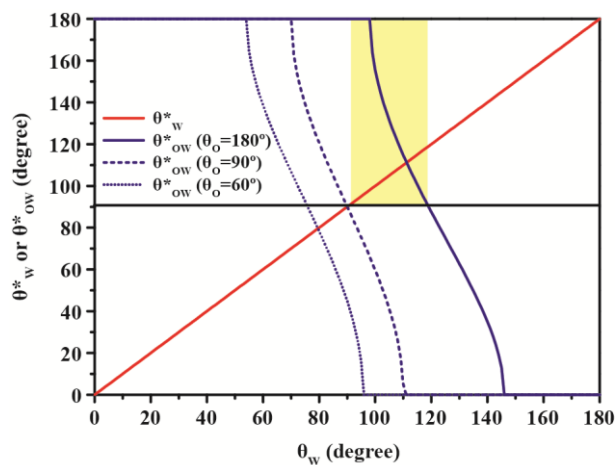


Figure S58. Dependency of θ^*_W (red line) and θ^*_{OW} (blue lines) on θ_W when f is 1.

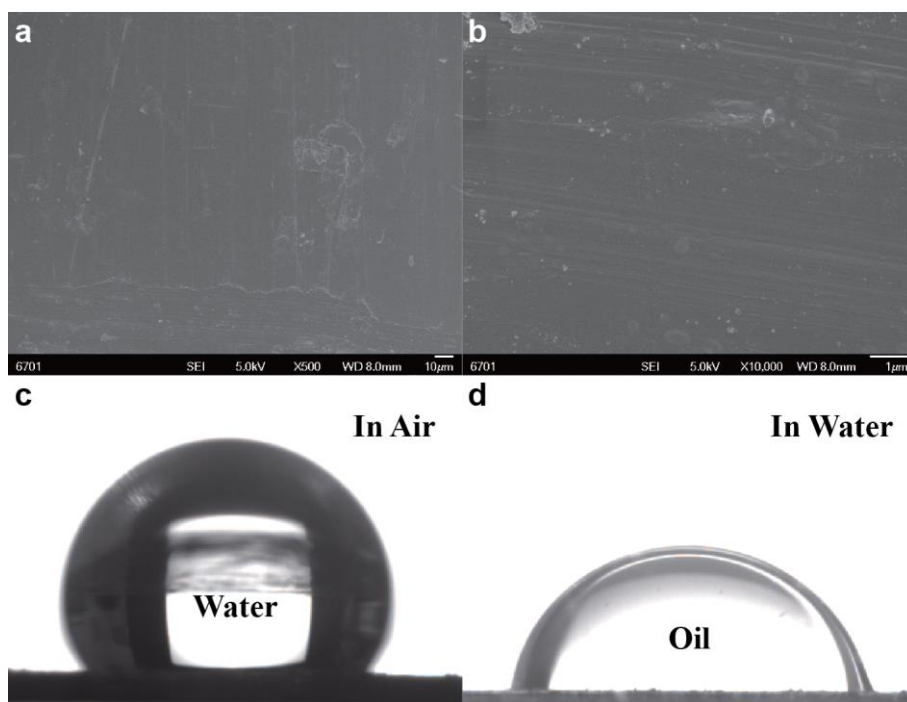


Figure S59. (a, b) SEM images, (c) θ^*_W , and (d) θ^*_{OW} of original flat copper sheet modified with 0.2 mM 1H,1H,2H,2H-perfluorodecanethiol.

Movie S1. θ^*_w of CuO-coated fabric.

Movie S2. θ^*_w of CuO-coated fabric modified with 0.1 mM n-octadecylthiol.

Movie S3. Sliding angles of the dual superlyophobic fabric.

Movie S4. Separation of hexane-water mixture using the dual superlyophobic fabric.

Movie S5. Separation of dichloroethane-water mixture using the dual superlyophobic fabric.